
Are Your Generated Instances Truly Useful?

GenBench-MILP: A Benchmark Suite for MILP Instance Generation

Yidong Luo¹ Chenguang Wang¹ Dong Li² Tianshu Yu¹

Abstract

The proliferation of machine learning-based methods for Mixed-Integer Linear Programming (MILP) instance generation has surged, driven by the need for diverse training datasets. However, a critical question remains: Are these generated instances truly useful and realistic? Current evaluation protocols often rely on superficial structural metrics or simple solvability checks, which frequently fail to capture the true computational complexity of real-world problems. To bridge this gap, we introduce GenBench-MILP, a comprehensive benchmark suite designed for the standardized and objective evaluation of MILP generators. Our framework assesses instance quality across four key dimensions: mathematical validity, structural similarity, computational hardness, and utility in downstream tasks. A distinctive innovation of GenBench-MILP is the analysis of solver-internal features—including root node gaps, heuristic success rates, and cut plane usage. By treating the solver’s dynamic behavior as an expert assessment, we reveal nuanced computational discrepancies that static graph features miss. Our experiments on instance generative models demonstrate that instances with high structural similarity scores can still exhibit drastically divergent solver interactions and difficulty levels. By providing this multifaceted evaluation toolkit, GenBench-MILP aims to facilitate rigorous comparisons and guide the development of high-fidelity instance generators. The code is available in <https://github.com/Aux-724/GenBench-MILP>

gramming (LP) by incorporating integer variables, enabling the modeling of discrete decisions and logical conditions often intractable with purely continuous models (Achterberg & Wunderling, 2013; Wolsey, 2020). Its versatility in capturing complex relationships like fixed costs, mutual exclusivity, and indivisible entities makes MILP essential for practical decision-making in fields such as supply chain optimization, scheduling, financial modeling, and network design (Hugos, 2018; Branke et al., 2015; Mansini et al., 2015; Al-Falahy & Alani, 2017).

Traditionally, MILP solver advancement relied on benchmark libraries like MIPLIB (Gleixner et al., 2021) and other real-world instance collections. *However, these static benchmarks often lack the scalability, diversity, or controllable characteristics vital for modern research.* These limitations are particularly acute with the rise of machine learning (ML) in optimization, where learning-based approaches for tasks like branching strategy selection or algorithm configuration demand large, varied datasets that often exceed available collections (Bengio et al., 2021). Consequently, a significant shift towards proactive **generation of MILP instances** has occurred (Bowly et al., 2020; Geng et al., 2023; Wang et al., 2023; Guo et al., 2024; Liu et al., 2024; Yang et al., 2024a; Zeng et al., 2024; Zhang et al., 2024). This trend towards instance generation is motivated by multiple highlighted advantages: fulfilling the need for extensive datasets in ML applications; achieving greater instance diversity than found in existing libraries (Gleixner et al., 2021); enabling control over computational difficulty for rigorous algorithm testing; facilitating the simulation of specific problem structures (Liu et al., 2024); aiding solver testing and debugging (Gurobi Optimization LLC, 2021); and creating privacy-preserving surrogates for confidential real-world data.

1. Introduction

Mixed-Integer Linear Programming (MILP) is a fundamental optimization framework extending standard Linear Pro-

¹School of Data Science, The Chinese University of China, Shenzhen ²Huawei. Correspondence to: Tianshu Yu <yutianshu@cuhk.edu.cn>.

Methodologies for MILP instance generation have evolved in tandem. Early approaches featured parameterized generators for **specific problem classes** such as the traveling salesman problems (Pilcher & Rardin, 1992; Vander Wiel & Sahinidis, 1995), set covering (Balas & Ho, 1980), or quadratic assignment problems (Culberson, 2002). Later techniques emphasized more **generalized feature-based descriptions** and **sampling** (Bowly et al., 2020; Smith-Miles & Bowly, 2015). Most recently, **deep learning based frameworks** like G2MILP (Geng et al., 2023), MILP-StuDio

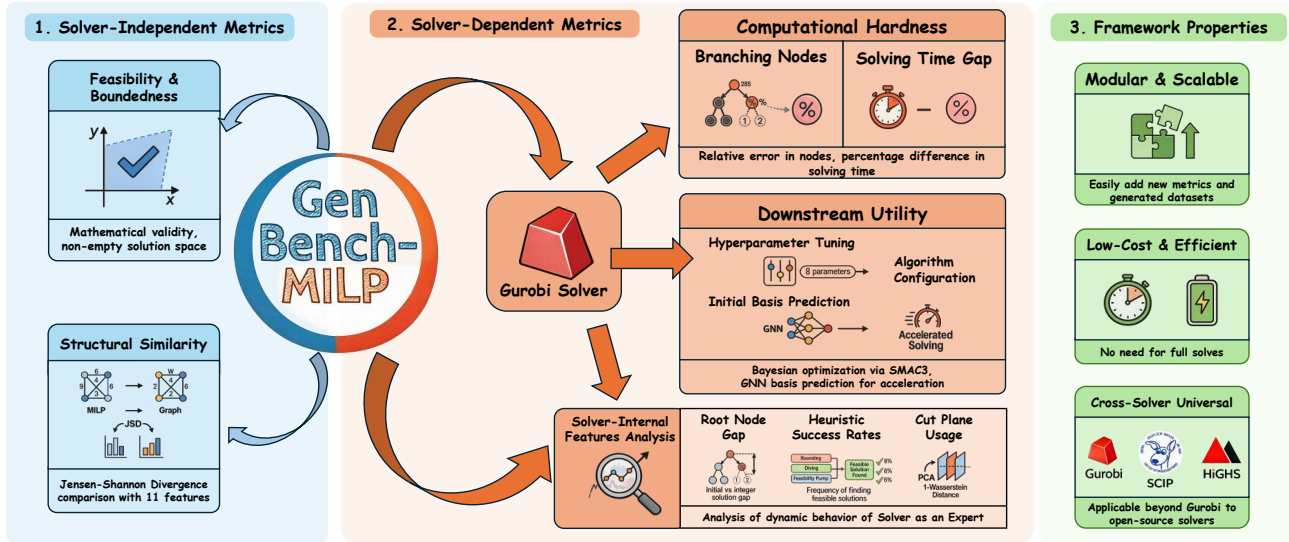


Figure 1. Architecture of GenBench-MILP

(Liu et al., 2024), and MILP-Evolve (Li et al., 2024) have gained prominence. These often represent MILP instances as graphs (e.g., bipartite graphs) and use **generative models** like variational autoencoders (Kipf & Welling, 2016) to learn and replicate specific structures from training data, *marking a significant potential advancement but also introducing new evaluation challenges*. More information about related work could be found in Appendix B

Despite this progress in generation, a critical and multi-faceted challenge remains: the fair, objective, and comprehensive evaluation of synthetic MILP instance “quality”. Assessing generator outputs effectively requires considering several dimensions: **(I) Ensuring fundamental solvability** (feasibility and boundedness) is crucial yet non-trivial (Wang et al., 2023; Geng et al., 2023; Liu et al., 2024). **(II) Generated instances should ideally mirror real-world structural patterns** (Gleixner et al., 2021), *but mere resemblance may not capture true computational behavior*. **(III) Instances must exhibit appropriate and controllable computational hardness**, typically evaluated via solver performance (Gurobi Optimization LLC, 2021), though achieving desired hardness levels consistently is a significant difficulty. Furthermore, *current evaluation protocols* (Geng et al., 2023; Bowly et al., 2020; Zhang et al., 2024) *often lack standardization, hindering robust comparisons and impeding progress*.

To address the lack of a standardized and comprehensive methodology for evaluating MILP instance generation techniques, this research introduces a novel benchmark framework. Our unified and extensible framework assesses instance quality across key dimensions – mathematical va-

lidity, structural similarity, computational hardness, solver interaction patterns, and utility for downstream ML tasks. By establishing an objective standard, we aim to facilitate fairer comparisons, guide the development of higher-quality generators, and improve the reliability of research utilizing synthetic MILP data. The **practical viability** and **robustness** of our framework is confirmed by our tests on the super hard dataset with a strict 120-second time limit, *proving our solver-internal features are highly stable and confirming the approach is both low-cost and efficient*. Our experiments on open-source solvers SCIP and HIGHS further confirm that *while the framework is general, state-of-the-art solvers like Gurobi yield more precise internal features*. These findings not only validate our framework but also highlight a limitation in current DL-based generation approaches. While representing MILP instances as bipartite graphs has enabled progress in achieving structural similarity, this representation may struggle to fully capture the intricate constraint relationships and inherent mathematical properties crucial for MILP feasibility and hardness. We posit that future advancements might benefit from shifting focus from direct graph structure manipulation towards methods that more directly model the underlying mathematical structure or solution space characteristics. The proposed benchmark provides the necessary tools to rigorously evaluate such novel approaches.

Our specific contributions are four-fold: **(I)** We integrate both **Solver-Independent Metrics** (covering fundamental properties and structural resemblance) and **Solver-Dependent Metrics** (including computational characteristics and downstream task utility) for a holistic assessment. **(II)** We incorporate detailed analysis of **solver-internal**

features (e.g., **root node gap**, **heuristic success counts**, **cut plane profiles**), using the solver’s behavior as an expert assessment to reveal deeper computational similarities. **(III)** The framework is designed for **extendability**, featuring a modular structure to easily accommodate new metrics, datasets, and generation techniques over time. **(IV)** We provide the community with clear, operational metrics and quantitative criteria to objectively benchmark diverse generator types (e.g., rule-based, statistical, and machine learning-based), thereby steering future development.

2. Preliminaries

MILP and its Bipartite Graph Representation. We consider the standard MILP problem:

$$\min_{\mathbf{x} \in \mathbb{R}^n} \tilde{\mathbf{c}}^\top \mathbf{x}, \quad \text{s.t.} \quad \mathbf{A}\mathbf{x} \leq \mathbf{b}, \quad x_i \in \mathbb{Z}, \quad \forall i \in \mathcal{I}.$$

Here, \mathbf{x} is the vector of decision variables, $\tilde{\mathbf{c}}$ contains the objective coefficients, \mathbf{A} is the constraint matrix, \mathbf{b} is the vector of constraint bounds, and \mathcal{I} identifies the integer variables.

Representing MILP instances as weighted bipartite graphs is an established practice in the relevant literature (Zhang et al., 2023; Gasse et al., 2019; Nair et al., 2021). In this common representation, each MILP instance corresponds to a graph \mathcal{G} defined by three sets: constraint vertices \mathcal{C} , variable vertices \mathcal{V} , and edges \mathcal{E} connecting them. The constraint partition $\mathcal{C} = \{c_1, \dots, c_m\}$ includes one vertex c_i for each of the m constraints, where the vertex feature c_i typically represents the bias term, i.e., $c_i = (b_i)$ (the i -th element of \mathbf{b} from the MILP formulation). The variable partition $\mathcal{V} = \{v_1, \dots, v_n\}$ contains one vertex v_j for each of the n variables, with the corresponding 9-dimensional feature vector \mathbf{v}_j encoding information such as the objective coefficient c_j (from the MILP vector \mathbf{c}), the variable type, and the bounds l_j, u_j (from the MILP vectors \mathbf{l} and \mathbf{u}). Edges in \mathcal{E} only exist between vertices from different partitions ($c_i \in \mathcal{C}$ and $v_j \in \mathcal{V}$). An edge $e_{i,j}$ connects c_i and v_j if the corresponding element $A_{i,j}$ in the constraint matrix \mathbf{A} is non-zero; its associated feature $e_{i,j}$ is described by this coefficient, i.e., $e_{i,j} = (A_{i,j})$. If $A_{i,j}$ is zero, the edge $e_{i,j}$ is considered absent.

Linear Programming Relaxation. Given the MILP problem:

$$z_{\text{MILP}} = \min_{\mathbf{x}} \{\tilde{\mathbf{c}}^\top \mathbf{x} \mid \mathbf{A}\mathbf{x} \leq \mathbf{b}, x_i \in \mathbb{Z} \forall i \in \mathcal{I} \subseteq \{1, \dots, n\}\}.$$

The *LP relaxation* is obtained by omitting the integrality constraints:

$$z_{\text{LP}} = \min_{\mathbf{x}} \{\tilde{\mathbf{c}}^\top \mathbf{x} \mid \mathbf{A}\mathbf{x} \leq \mathbf{b}\}.$$

Let $\mathcal{P} = \{\mathbf{x} \in \mathbb{R}^n \mid \mathbf{A}\mathbf{x} \leq \mathbf{b}\}$ be the feasible region of the LP relaxation. The optimal objective value of the

LP relaxation provides a lower bound (for minimization problems) to the optimal objective value of the original MILP, i.e., $z_{\text{LP}} \leq z_{\text{MILP}}$.

Duality Gap. In the context of solving the MILP $\min \tilde{\mathbf{c}}^\top \mathbf{x}$, the *duality gap* measures the difference between the objective value of the best known feasible integer solution, $z_{\text{incumbent}}$ (primal bound or upper bound, UB), and the best proven objective bound, z_{bound} (dual bound or lower bound, LB), typically derived from LP relaxations ($z_{\text{bound}} \geq z_{\text{LP}}$). The absolute gap is $G_{\text{abs}} = z_{\text{incumbent}} - z_{\text{bound}}$ (assuming $z_{\text{incumbent}} \geq z_{\text{bound}}$). The relative gap, often used as a termination criterion, quantifies the remaining gap relative to one of the bounds, e.g.:

$$G_{\text{rel}} = \frac{z_{\text{incumbent}} - z_{\text{bound}}}{\max(1, |z_{\text{incumbent}}|)}.$$

Optimality is proven when $z_{\text{incumbent}} = z_{\text{bound}}$, or G_{abs} (or G_{rel}) is within a predefined tolerance $\epsilon \geq 0$.

Feasibility Consider the MILP problem defined by constraints $\mathbf{A}\mathbf{x} \leq \mathbf{b}$ and $x_i \in \mathbb{Z}, \forall i \in \mathcal{I}$. The feasible region is the set $\mathcal{F} = \{\mathbf{x} \in \mathbb{R}^n \mid \mathbf{A}\mathbf{x} \leq \mathbf{b}, x_i \in \mathbb{Z} \forall i \in \mathcal{I}\}$. The MILP problem is *feasible* if its feasible region \mathcal{F} is non-empty, i.e., $\mathcal{F} \neq \emptyset$. A specific point $\hat{\mathbf{x}} \in \mathbb{R}^n$ is considered *feasible* if it satisfies all constraints, i.e., $\hat{\mathbf{x}} \in \mathcal{F}$.

Boundedness Given the MILP objective $\min_{\mathbf{x} \in \mathcal{F}} \tilde{\mathbf{c}}^\top \mathbf{x}$, the problem is *bounded* if the optimal objective value z^* is finite. This means $z^* = \inf_{\mathbf{x} \in \mathcal{F}} \tilde{\mathbf{c}}^\top \mathbf{x} > -\infty$. (For a maximization problem $\max_{\mathbf{x} \in \mathcal{F}} \tilde{\mathbf{c}}^\top \mathbf{x}$, boundedness would mean $z^* = \sup_{\mathbf{x} \in \mathcal{F}} \tilde{\mathbf{c}}^\top \mathbf{x} < +\infty$). If a problem is both feasible ($\mathcal{F} \neq \emptyset$) and bounded, a finite optimal objective value z_{MILP} exists.

Additional preliminaries can be found in Appendix E.

3. Methodology

This section outlines the methodology employed to evaluate the quality and characteristics of generated MILP instances. We compare instances generated using reproductions of three open-source methods – G2MILP (Geng et al., 2023), ACM-MILP (Guo et al., 2024), and DIG-MILP (Wang et al., 2023) – against a baseline set of ‘original’ instances. This baseline set, comprising Set Cover, Combinatorial Auction (CA), Capacitated Facility Location (CFL), and Independent Set (IS) problems, was synthesized using the Ecole library (Prouvost et al., 2020) (the specific parameter settings used for this synthesis are detailed in the Appendix A.1), while IP and LB come from two challenging real-world problem families used in ML4CO 2021 competition (Gasse et al., 2022). To capture different facets of similarity and fidelity between the generated and original sets, we utilize a suite of metrics. These metrics are organized into two primary categories based on their reliance on the underlying opti-

mization solver: **(I) Solver-Independent Metrics**, which assess inherent properties of the MILP instances themselves (e.g., feasibility, structure) without regard to any specific solution process; and **(II) Solver-Dependent Metrics**, which evaluate aspects intrinsically linked to the behavior and performance of a particular solver (primarily Gurobi) when applied to the instances. This dual approach allows for a robust assessment, considering both fundamental instance properties and their practical implications for optimization algorithms (See the whole framework in Figure 1).

3.1. Datasets

This study evaluates MILP instances from two sources: original instances (baselines and validation) and those from three generative models (G2MILP, ACM-MILP, DIG-MILP). Baselines include four synthetic datasets (SC, CA, CFL, IS) from Ecole (Prouvost et al., 2020) (details in Appendix A.1) and public benchmarks from the ML4CO Competition 2024 (Gasse et al., 2022) for pipeline validation. Due to the inherent specialization of current generative models to particular problem types, our comparative analysis specifically examines SC instances from G2MILP, CA instances from ACM-MILP and DIG-MILP, and IS instances from ACM-MILP and G2MILP. We emphasize that these specific combinations serve primarily as representative examples to demonstrate the utility of our metrics; the GenBench-MILP framework itself is dataset-agnostic, and its broader applicability to other distinct datasets and models has been confirmed (see Section 4.1).

3.2. Solver-Independent Metrics

3.2.1. FEASIBILITY RATIO

This metric measures the proportion of instances that are both **feasible** and **bounded**. Most methods maintain near-perfect feasibility across datasets, with only minor exceptions (e.g., G2MILP on MIS at $\eta = 0.10$). Detailed results are given in Table 12 in the Appendix.

3.2.2. STRUCTURAL SIMILARITY

To quantitatively assess the **structural similarity** between two sets of MILP instances, following (Geng et al., 2023), we implemented a feature-based comparison method. Each instance is first converted into a graph representation, from which a vector of **11 predefined structural features** is extracted. For each feature, we compute the **Jensen-Shannon Divergence (JSD)** between the distributions of the two sets and transform it into a similarity score $S_i = 1 - \frac{JSD_i}{\log(2)}$, where a score of 1 indicates identical distributions and 0 indicates maximal divergence. The overall structural similarity between the two sets is the arithmetic mean of these feature scores. Overall, the JSD-based metric (Ta-

Table 1. Structural Similarity. The similarity score is derived from Jensen-Shannon Divergence (higher is better). The **Masked Ratio** (η) denotes the proportion of the original instance’s structure (e.g., constraint nodes in G2MILP or constraints in ACM-MILP) that is masked, corrupted, or selected for reconstruction during the generation process, serving as a control parameter for the modification magnitude.

Problem	Model	Similarity at Masked Ratio (η)			
		0.01	0.05	0.10	0.20
CA	ACM-MILP	—	0.889	0.867	0.892
CA	DIG-MILP	0.861	0.860	0.879	—
IS	ACM-MILP	—	0.734	0.731	0.699
IS	G2MILP	0.486	0.473	0.466	—
SC	G2MILP	0.990	0.950	0.921	—

ble 1) indicates that ACM-MILP and DIG-MILP closely match the structural characteristics of CA data (around 0.86–0.89), while ACM-MILP achieves moderate similarity on IS (around 0.70) and G2MILP is lower (around 0.47). For Set Cover, G2MILP performs best, reaching very high similarity (around 0.92–0.99), especially at lower mask ratios.

3.3. Solver-Dependent Metrics

3.3.1. BRANCHING NODES

Computational hardness is measured by the number of **branch-and-bound nodes** explored by Gurobi, using the relative error $\left| \frac{\sum Nodes_{gen} - \sum Nodes_{train}}{\sum Nodes_{train}} \right| \times 100\%$. As shown in Table 2 (Appendix F), hardness varies strongly by model and problem type: G2MILP on IS can exceed 50,000 % RE and often times out, ACM-MILP on CA reaches over 26,000 % RE, while DIG-MILP and other settings remain closer to baseline.

3.3.2. SOLVING TIME GAP

This metric measures the percentage difference in average solving times between generated and original instances, where smaller gaps indicate closer solver-conditional hardness. Table 14 in Appendix shows that G2MILP for SC keeps gaps modest (≈ 11 – 22%), DIG-MILP for CA remains near baseline (≈ 20 – 29%), while ACM-MILP can greatly alter hardness (e.g., 2400%+ increase for CA or ~ 47 – 49% faster for IS).

3.3.3. HYPERPARAMETER TUNING

Automatically optimizing solver hyperparameters is known to be crucial for achieving peak performance on complex algorithms like MILP solvers (Hutter et al., 2011). Therefore, we employed the Sequential Model-based Algorithm Configuration (**SMAC3**) framework (Lindauer et al., 2022),

Table 2. Branching Node Statistics and Relative Error across Problem Types. Statistics are calculated over 1000 instances per source/ratio. **Original** refers to the original training sets (Total Nodes: IS=14,255; CA=18,488; SC=46,408). 'Time Limit Hits' indicates premature termination. Relative Error (RE) compares generated total nodes to baseline total nodes. η denotes the mask ratio.

Problem	Source	Mask Ratio (η)	Mean Nodes	Median Nodes	Std Dev	Max Nodes	Time Limit Hits	Relative Error (%)	
IS	Original	N/A	14.3	1.0	49.1	1,056	0	—	
	G2MILP	0.01	26.2	1.0	60.1	724	0	84.1	
	G2MILP	0.05	765.7	175.0	1,941.6	16,314	5	5,271.6	
	G2MILP	0.10	8,386.4	8,330.0	1,219.5	11,789	982	58,730.0	
	ACM-MILP	0.05	8.8	1.0	36.8	572	0	38.3	
	ACM-MILP	0.10	10.9	1.0	63.8	1,344	0	23.4	
	ACM-MILP	0.20	12.5	1.0	78.0	1,977	0	12.3	
	CA	Original	N/A	18.5	1.0	48.1	514	0	—
	ACM-MILP	0.05	6,556.0	1,661.5	9,926.3	51,913	138	35,360.0	
	ACM-MILP	0.10	6,504.9	1,547.0	9,962.8	54,385	120	35,084.3	
ACM-MILP	0.20	4,873.6	962.5	8,021.7	43,036	75	26,259.8		
DIG-MILP	DIG-MILP	0.01	34.1	1.0	76.2	799	0	84.4	
	DIG-MILP	0.05	34.3	1.0	76.4	812	0	85.6	
	DIG-MILP	0.10	37.8	1.0	83.5	902	0	104.3	
	SC	Original	N/A	46.4	1.0	298.6	8,135	0	—
G2MILP	0.01	85.4	1.0	536.5	14,592	0	84.0		
G2MILP	0.05	79.6	1.0	430.9	10,643	0	71.6		
G2MILP	0.10	63.7	1.0	269.8	4,713	0	37.3		

which utilizes Bayesian optimization. Following the approach in (Liu et al., 2024), the tuning process targeted **8 key Gurobi parameters**. These parameters were selected as they govern diverse and fundamental components of the MILP solution process, including primal heuristics, search strategy focus, branching decisions, presolving routines, cutting plane generation, and node LP solution methods. The significant impact of these core solver components, and thus the parameters controlling them, on overall performance is well-documented in the MILP literature (e.g., Lodi & Zarpellon, 2017; Achterberg, 2009; Berthold, 2012). The objective function for SMAC3 was the minimization of the mean wall-clock solve time across the instances within a designated tuning set. The primary goal of this hyperparameter tuning experiment was to evaluate the **generalization** capability of the optimized Gurobi configurations using generated MILP instances. SMAC3 tuning (Table 3) gives model- and dataset-specific gains. ACM-MILP (IS) decreases about **10%** at $\eta = 0.1$. DIG-MILP (CA) consistently cuts time by about **61%**, and G2MILP (SC) by about **44%**, while the original SC set improves only about **3%**.

3.3.4. INITIAL BASIS PREDICTION

Following the methodology of (Fan et al., 2023), we investigated predicting an **initial basis** for MILP relaxations using a GNN. While adhering to the principles outlined by Fan et al., our implementation was developed independently from scratch. For this purpose, a GNN model was trained specifically on generated MILP instances to predict the basis status (basic or non-basic at lower/upper bounds) for variables and slack variables associated with the MILP relaxation. The

Table 3. Solving time improvement after Gurobi hyperparameter tuning. Compares the average wall-clock time (seconds) on the test set for the default configuration versus the best configuration found by SMAC3.

Dataset	Source	η	Default(s)	Best(s)	Improv. (%)
IS	ACM-MILP	0.05	0.339	0.370	-9.17
		0.1	0.351	0.280	20.25
		0.2	0.339	0.377	-11.13
	Original	—	0.336	0.366	8.98
CA	DIG-MILP	0.01	0.107	0.041	61.35
		0.05	0.109	0.042	61.63
		0.1	0.108	0.042	61.38
	Original	—	0.107	0.042	61.26
SC	G2MILP	0.01	0.211	0.118	43.97
		0.05	0.211	0.118	44.06
		Original	—	0.229	0.221

GNN’s predictions were subsequently refined into a numerically stable basis using established techniques. To evaluate the effectiveness of training on generated data versus original data for this task, we measured the impact of using the initial basis predicted by the GNN on Gurobi’s performance metrics (solving time, runtime). This was compared against Gurobi’s default setting and potentially a model trained on original data, using unseen test instances. The validity and effectiveness of our re-implemented approach are substantiated by the experimental outcomes. Results are in Table 4.

Table 4. Impact of Generative Data Augmentation on GNN Initial Basis Prediction. This table evaluates the solving time improvement achieved by initializing Gurobi with a GNN-predicted basis compared to the default initialization. The GNN models were trained either on the **Original** dataset alone or on the original dataset augmented with synthetic instances generated by different **Sources**. All performance metrics (average runtime in seconds) are measured on the unseen original test set. **Default:** Gurobi’s default runtime; **Best:** Runtime using the GNN-predicted basis; **Improv.:** Percentage reduction in runtime relative to the default.

Dataset	Source	η	Default (s)	Best (s)	Improv. (%)
CA	ACM-MILP	0.05	0.078	0.077	2.6%
		0.10	0.079	0.076	2.6%
		0.20	0.078	0.075	4.0%
	DIG-MILP	0.05	0.079	0.076	3.5%
		0.10	0.080	0.076	4.1%
		Original	—	0.078	0.077
IS	ACM-MILP	0.10	0.236	0.239	-0.2%
	G2MILP	0.05	0.237	0.240	-0.6%
	Original	—	0.236	0.237	0.2%
SC	G2MILP	0.01	0.236	0.221	10.6%
		0.05	0.240	0.229	9.1%
		0.10	0.242	0.224	12.4%
	Original	—	0.236	0.226	9.1%

3.3.5. SOLVER-INTERNAL FEATURES

We introduce a novel, computationally efficient methodology to evaluate MILP instance fidelity using **solver-internal features**: metrics from Gurobi’s deterministic solving process. We first validated the solver-internal-feature methodology via a split-half experiment (see Appendix K.1). Figure 2 shows one representative result, where random original-set subsets exhibit very low **1-Wasserstein distances** (e.g. 0.130 for heuristic, 0.188 for root-node gap, 0.232 for cut-plane profiles), confirming its ability to capture authentic inter-set similarity. To further demonstrate practical viability, we applied the method to the **hard** ML4CO *item_placement* dataset under a strict 120-second limit (see more in Section 4.1). This shows that we do not need to fully solve the instance to extract the features. Solver-internal features extracted from Gurobi proved stable and inexpensive to compute. What’s more, comparison with experiments of open-source solvers **SCIP** and **HiGHS** (see more in Section 4.2) indicates that, although the framework is general, state-of-the-art solvers like Gurobi provide more precise internal metrics.

Table 5. Comparison of Root Node Gap Distributions

Problem	Model	η	Mean Gap (%)		Std Dev (%)		W_1 Dist.
			Gen	Original	Gen	Original	
CA	DIG-MILP	0.01	1.11	2.47	1.22	2.60	1.3001
		0.05	1.09	2.47	1.17	2.60	1.3787
		0.10	1.18	2.47	1.26	2.60	1.2982
	ACM-MILP	0.05	7.93	2.47	3.85	2.60	5.4638
		0.10	7.49	2.47	3.60	2.60	5.0187
		0.20	9.54	2.47	4.40	2.60	7.0666
IS	ACM-MILP	0.05	2.65	3.42	1.82	1.34	0.8818
		0.10	2.66	3.42	1.81	1.34	0.8646
		0.20	2.45	3.42	1.80	1.34	1.0388
SC	G2MILP	0.01	8.25	7.61	4.19	4.12	0.6690
		0.05	7.75	7.61	4.27	4.12	0.2294
		0.10	8.05	7.61	4.12	4.12	0.5103

With fixed Gurobi settings, we extracted: **Root Node Gap**, **Heuristic Success Count**, and **Cut Plane Usage vectors**. Distributions for Root Node Gap and Heuristic Success Count were compared using the 1-Wasserstein distance (W_1). For Cut Plane Usage, per-instance vectors were pre-processed, underwent PCA, and distributions of scores on dominant principal components were then compared using the W_1 distance.

Results Table 5 presents W_1 distances for root gap distributions (lower W_1 indicates higher similarity). G2MILP highly replicated SC root gaps (e.g., $W_1 = 0.2294$ at $\eta = 0.05$). In contrast, DIG-MILP and ACM-MILP significantly diverged for CA. ACM-MILP showed moderate success for IS at lower η , diminishing as η increased.

For primal heuristic success distributions (Table 6, W_1 dis-

Table 6. Comparison of Heuristic Success Frequency Distributions

Problem	Model	η	Gen. Stats		Base Stats		W_1 Dist.
			Mean	Std	Mean	Std	
CA	ACM-MILP	0.05	2.549	0.500	2.115	0.379	0.434
		0.10	2.552	0.501	2.115	0.379	0.437
		0.20	2.457	0.500	2.115	0.379	0.342
	DIG-MILP	0.01	2.238	0.451	2.115	0.379	0.135
		0.05	2.241	0.439	2.115	0.379	0.126
		0.10	2.258	0.440	2.115	0.379	0.143
IS	ACM-MILP	0.05	1.662	0.473	18.883	12.112	17.221
		0.10	1.746	0.435	18.883	12.112	17.137
		0.20	1.849	0.358	18.883	12.112	17.034
SC	G2MILP	0.01	2.619	0.533	2.702	0.491	0.083
		0.05	2.600	0.548	2.702	0.491	0.102
		0.10	2.598	0.541	2.702	0.491	0.104

Table 7. Comparison of Cutting Plane Usage Distributions

Problem	Model	η	Wasserstein Distance		
			PC1	PC2	PC3
CA	ACM-MILP	0.05	1.5570	0.8352	0.5349
		0.10	1.4837	0.7155	0.3570
		0.20	1.6889	0.3166	0.3731
	DIG-MILP	0.01	1.4711	0.6673	0.3601
		0.05	1.4868	0.6826	0.3047
		0.10	1.5392	0.4394	0.5988
IS	ACM-MILP	0.05	0.8944	0.4986	0.2517
		0.10	0.9354	0.3942	0.0963
		0.20	1.0097	0.5735	0.1199
SC	G2MILP	0.01	0.0707	0.1271	0.1124
		0.05	0.1714	0.1425	0.0677
		0.10	0.1374	0.1028	0.1375

tance), DIG-MILP (e.g., $W_1 \approx 0.14$) and ACM-MILP (e.g., $W_1 \approx 0.34 - 0.44$) achieved good similarity for CA problems. G2MILP (SC) demonstrated remarkable similarity ($W_1 \approx 0.08 - 0.10$). Conversely, ACM-MILP (IS) instances diverged significantly ($W_1 \approx 17.0 - 17.2$).

For cutting plane usage (Table 7), G2MILP (SC) achieved the highest similarity (e.g., PC1 $W_1 \approx 0.07 - 0.17$). In contrast, ACM-MILP and DIG-MILP for CA instances showed significant divergences (DIG-MILP PC1 $W_1 \approx 1.47 - 1.69$). ACM-MILP (IS) demonstrated intermediate similarity (PC1 $W_1 \approx 0.89 - 1.01$).

4. Experiments

4.1. Efficiency Test on Super Hard Instances

To validate the practical feasibility and robustness of our solver-internal feature analysis method, we designed an efficiency test. The core goal of this experiment is to demon-

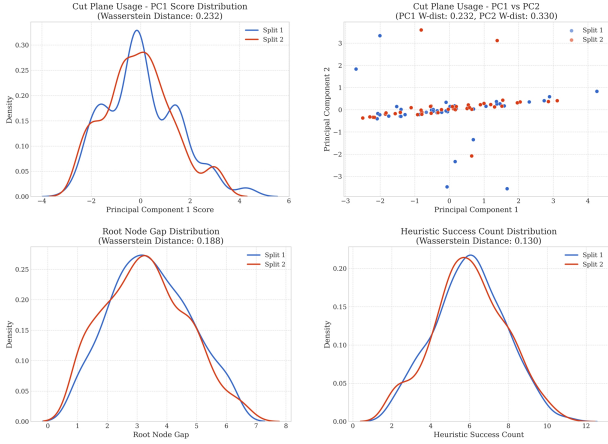


Figure 2. Internal Cut-plane Comparison of IS (Demonstration of Identical Distribution)

strate that even under strict computational constraints (i.e., tight time limits) and when facing a well-known set of hard instances, our method can still stably and efficiently extract meaningful feature distributions. This supports our key hypothesis that obtaining such deep behavioral features does not require solving instances to optimality, thereby making the evaluation both low-cost and highly efficient.

Table 8. W-1 distances of solver-internal features across item placement halves

Feature	W-1 Dist.
Root Node Gap	0.7613
Heuristic Success Count	0.7320
Cut Plane Usage	
– PC1	0.0917
– PC2	0.0870
– PC3	0.0904

Dataset Selection: We used the item placement dataset from the ML4CO competition, which is recognized for its high solving difficulty. A total of 1000 instances were selected for testing.

Computational Budget Constraint: To simulate scenarios with limited computational resources, we imposed a strict time limit of **120 seconds** for the Gurobi solver on each instance.

Validation Method: We employed a split-half validation approach to evaluate the stability of the extracted features. The 1000 solver logs were randomly divided into two halves of 500 instances each. We then independently extracted solver-internal features—including Root Node Gap, Heuristic Success Count, and Cut Plane Usage—from both halves and computed the distributional similarity between them. Strong stability and reliability of the extraction method are

indicated if these random subsets, originating from the same underlying distribution, exhibit highly similar feature distributions (i.e., a low Wasserstein distance).

The split-half validation demonstrates remarkable stability in the extracted solver-internal features, even under the strict 120-second time limit. As shown in Table 8, the Cut Plane Usage metric exhibits exceptionally low 1-Wasserstein distances for its top three principal components (PC1: 0.0917, PC2: 0.0870, and PC3: 0.0904). These near-zero values indicate that the solver’s strategic application of cuts—a crucial early-stage behavior—is highly consistent across the two random data subsets. Similarly, the Root Node Gap (0.7613) and Heuristic Success Count (0.7320) show strong distributional similarity, confirming that a stable signal for these metrics can also be captured long before the solver reaches optimality. Collectively, these results validate that a truncated solving process is sufficient to extract a reliable and consistent “fingerprint” of solver behavior, confirming the low-cost and efficient nature of our methodology.

Conclusion: This experiment strongly demonstrates the practical value of our framework: ① **High Efficiency and Low Cost:** The results confirm that a truncated solving process (120-second timeout) is sufficient to extract stable and representative solver-internal feature distributions. This substantially reduces the time and computational cost of evaluating large-scale or extremely hard instance sets. ② **Feature Stability:** The very small Wasserstein distances observed for Root Node Gap and Cut Plane Usage indicate that these early-stage solver behavior features are highly stable. ③ **Practical Feasibility:** The success of this test shows that the GenBench-MILP framework is not only theoretically sound but also practically applicable for evaluating MILP instances that are difficult to solve to optimality within a reasonable time frame and that reflect real-world complexity.

4.2. Cross-Solver Comparison and Stability Analysis

To assess the generality of the GenBench-MILP framework and probe the internal stability of different solvers, we extended our evaluation to include the open-source solvers SCIP and HiGHS. We conducted the same IS split-half validation procedure, using Gurobi as the stable baseline for comparison. Table 9 summarizes the key results.

Table 9. 1-Wasserstein distances across solvers on IS split-half validation

Feature	Gurobi (Baseline)	SCIP	HiGHS
Root Node Gap	0.1884	1.7530	26.7297
Heuristic (PC1)	0.1300	0.3190	0.2368
Cut Plane (PC1)	0.2318	0.7000	0.0612

The data reveals a complex and multi-faceted picture of solver stability. First, examining the **Root Node Gap**, we

observe dramatic differences. Gurobi exhibits exceptional stability with a Wasserstein distance of just **0.1884**. In stark contrast, HiGHS shows a distance of 26.7297, over **140 times** larger than Gurobi’s, signifying severe instability in its root node analysis. This suggests that the initial problem assessment and relaxation strategies in HiGHS are profoundly sensitive to small changes in problem structure. Second, the results for the primary principal component of **Heuristic** features show a similar trend, though less pronounced. Gurobi remains the most stable (0.1300), while SCIP and HiGHS are approximately **2.5x** and **1.8x** less stable, respectively. This implies Gurobi’s primal heuristic strategies are more robust. Interestingly, the analysis of **Cut Plane** features presents a contrasting result. Here, HiGHS is by far the most stable solver (0.0612), with a consistency nearly 4 times greater than Gurobi’s (0.2318). This suggests that HiGHS may employ a more deterministic or conservative cut generation strategy, whereas Gurobi and SCIP might use more adaptive, opportunistic approaches that are inherently more variable.

From this detailed analysis, we draw two main conclusions. First, the successful application to SCIP and HiGHS validates that *the GenBench-MILP framework is indeed solver-agnostic and generalizable*. Second, and more importantly, the quality of instance evaluation is intrinsically linked to solver stability, which is not monolithic but *highly feature-dependent*. Gurobi’s superior stability in the critical root-node phase makes it the most reliable choice for a baseline. The extreme volatility of the root node gap in HiGHS, for instance, could obscure subtle computational similarities that a more stable solver like Gurobi can reliably detect.

In summary, this cross-solver comparison highlights a powerful secondary application of our framework. Beyond its primary purpose of instance evaluation, *GenBench-MILP serves as an effective diagnostic tool for profiling the internal dynamics of MILP solvers*, offering quantitative insights into their stability and behavioral responses to perturbations across different strategic components.

5. Discussion

Finding 1: *Superficial structural similarity is an unreliable predictor of computational behavior and difficulty in generated MILP instances.* ACM-MILP (CA) instances showed high structural similarity but were exceptionally difficult to solve, with Root Node Gap discrepancies suggesting that structural metrics miss key complexity drivers or that models introduce subtle, difficulty-enhancing variations.

Finding 2: *Simple outcome metrics, such as solving time or branching nodes, do not adequately reveal the source of problem difficulty or underlying changes to instance*

structure. This is exemplified by ACM-MILP (IS) instances, which, despite some similar outcome metrics (e.g., solving time), exhibited vastly different heuristic behavior, indicating altered internal structures that impact solvability in ways not captured by these surface-level performance measures.

Finding 3: *The effectiveness of generative models is problem-dependent, linked to how well their modification strategies align with the core structural determinants of hardness for specific problem types.* G2MILP’s difficulty in generating realistic IS instances is likely due to IS problem hardness being rooted in global graph topology (Tarjan & Trojanowski, 1977; West, 2001), which its local edge constraint modifications struggle to preserve. G2MILP’s better performance on SC problems suggests its direct manipulation of constraint configurations (Balas & Ho, 1980) more effectively captures their structural hardness.

6. Conclusion

We introduce GenBench-MILP, a comprehensive benchmark framework designed to address the critical shortcomings of traditional evaluation methods for generated MILP instances. Our findings reveal that metrics based on superficial structural similarity or simple outcomes often fail to capture an instance’s true computational nature and difficulty. GenBench-MILP facilitates a more accurate and holistic assessment by shifting the focus towards solver-perceived difficulty and the practical utility of instances in downstream applications. By enabling this multifaceted methodology, our framework will be instrumental in guiding the development of higher-quality instance generators and fostering impactful research within the field of mathematical optimization.

Impact Statement

This paper presents work whose goal is to advance the field of Machine Learning. There are many potential societal consequences of our work, none which we feel must be specifically highlighted here.

References

- Achterberg, T. SCIP: solving constraint integer programs. *Mathematical Programming Computation*, 1(1):1–41, 2009.
- Achterberg, T. and Wunderling, R. *Mixed Integer Programming: Analyzing 12 Years of Progress*. Springer, 2013. doi: 10.1007/978-3-642-38189-8_18.
- Al-Falahy, N. and Alani, O. Y. Technologies for 5g networks: Challenges and opportunities. *IT Professional*, 19(1):12–20, 2017.

- Balas, E. and Ho, A. *Set Covering Algorithms Using Cutting Planes, Heuristics, and Subgradient Optimization: A Computational Study*. Springer, 1980.
- Bengio, Y., Lodi, A., and Prouvost, A. Machine learning for combinatorial optimization: A methodological tour d’horizon. *European Journal of Operational Research*, 290(2):405–421, 2021.
- Berthold, T. Primal heuristics for mixed integer programming. In *Mixed Integer Nonlinear Programming*, pp. 29–62. Springer, 2012.
- Bowly, S. et al. Generation techniques for linear programming instances with controllable properties. *Mathematical Programming Computation*, 12(3):389–415, 2020.
- Branke, J., Nguyen, S., Pickardt, C. W., and Zhang, M. Automated design of production scheduling heuristics: A review. *IEEE Transactions on Evolutionary Computation*, 20(1):110–124, 2015. doi: 10.1109/TEVC.2015.2429314.
- Conforti, M., Cornuéjols, G., and Zambelli, G. *Integer Programming*. Springer, 2014.
- Culberson, J. A graph generator for various classes of k-colorable graphs. URL <http://webdocs.cs.ualberta.ca/~joe/Coloring/Generators/generate.html>, 2002.
- Dantzig, G. B. *Linear Programming and Extensions*. Princeton University Press, 1963.
- Fan, Z. et al. Smart initial basis selection for linear programs. In *International Conference on Machine Learning*. PMLR, 2023.
- Gasse, M., Chételat, D., Ferroni, N., Charlin, L., and Lodi, A. Exact Combinatorial Optimization with Graph Convolutional Neural Networks, October 2019. URL <http://arxiv.org/abs/1906.01629>. arXiv:1906.01629 [cs, math, stat].
- Gasse, M., Bowly, S., Cappart, Q., Charfreitag, J., Charlin, L., Chételat, D., Chmiela, A., Dumouchelle, J., Gleixner, A., Kazachkov, A. M., Khalil, E., Lichocki, P., Lodi, A., Lubin, M., Maddison, C. J., Christopher, M., Papatgeorgiou, D. J., Parjadis, A., Pokutta, S., Prouvost, A., Scavuzzo, L., Zarpellon, G., Yang, L., Lai, S., Wang, A., Luo, X., Zhou, X., Huang, H., Shao, S., Zhu, Y., Zhang, D., Quan, T., Cao, Z., Xu, Y., Huang, Z., Zhou, S., Binbin, C., Minggui, H., Hao, H., Zhiyu, Z., Zhiwu, A., and Kun, M. The machine learning for combinatorial optimization competition (ml4co): Results and insights. In Kiela, D., Ciccone, M., and Caputo, B. (eds.), *Proceedings of the NeurIPS 2021 Competitions and Demonstrations Track*, volume 176 of *Proceedings of Machine Learning Research*, pp. 220–231. PMLR, Dec 2022. URL <https://proceedings.mlr.press/v176/gasse22a.html>.
- Geng, Z. et al. A deep instance generative framework for milp solvers under limited data availability. In *Advances in Neural Information Processing Systems*, volume 36, pp. 26025–26047, 2023.
- Gleixner, A., Hendel, G., Gamrath, G., Achterberg, T., Bastubbe, M., Berthold, T., Christophel, P., Jarck, K., Koch, T., Linderoth, J., et al. Miplib 2017: Data-driven compilation of the 6th mixed-integer programming library. *Mathematical Programming Computation*, 13(3): 443–490, 2021.
- Guo, Z. et al. Acn-milp: Adaptive constraint modification via grouping and selection for hardness-preserving milp instance generation. In *Forty-first International Conference on Machine Learning*, 2024.
- Gurobi Optimization LLC. Gurobi optimizer. URL <http://www.gurobi.com>, 2021. Accessed: DATE.
- Hugos, M. H. *Essentials of Supply Chain Management*. John Wiley & Sons, 2018. ISBN 978-1-119-46110-4.
- Hutter, F., Hoos, H. H., and Leyton-Brown, K. Sequential model-based optimization for general algorithm configuration. In *International Conference on Learning and Intelligent Optimization*, pp. 507–523. Springer, 2011.
- Kipf, T. N. and Welling, M. Variational graph auto-encoders. *arXiv preprint arXiv:1611.07308*, 2016.
- Li, S. et al. Towards foundation models for mixed integer linear programming. *arXiv preprint arXiv:2410.08288*, 2024.
- Lindauer, M., Eggenesperger, K., Feurer, M., Biedenkapp, A., Deng, D., Benjamins, C., Ruhkopf, T., Sass, R., and Hutter, F. Smac3: A versatile bayesian optimization package for hyperparameter optimization. *Journal of Machine Learning Research*, 23(54):1–9, 2022. URL <http://jmlr.org/papers/v23/21-0888.html>.
- Liu, H. et al. MILP-StuDio: MILP instance generation via block structure decomposition. *arXiv preprint arXiv:2410.22806*, 2024.
- Lodi, A. and Zarpellon, G. On the algorithmic effectiveness of modern MILP solvers. *Operations Research Perspectives*, 4:14–23, 2017.
- Mansini, R., Ogryczak, W., and Speranza, M. G. *Linear and Mixed Integer Programming for Portfolio Optimization*, volume 21. Springer, 2015. EURO: The Association of European Operational Research Societies.

- Nair, V., Bartunov, S., Gimeno, F., von Glehn, I., Lichocki, P., Lobov, I., O’Donoghue, B., Sonnerat, N., Tjandraatmadja, C., Wang, P., Addanki, R., Hapuarachchi, T., Keck, T., Keeling, J., Kohli, P., Ktena, I., Li, Y., Vinyals, O., and Zwols, Y. Solving mixed integer programs using neural networks. *arXiv preprint*, 2021.
- Pilcher, M. G. and Rardin, R. L. Partial polyhedral description and generation of discrete optimization problems with known optima. *Naval Research Logistics (NRL)*, 39(6):839–858, 1992.
- Prouvost, A., Dumouchelle, J., Scavuzzo, L., Gasse, M., Chételat, D., and Lodi, A. Ecole: A gym-like library for machine learning in combinatorial optimization solvers. In *Learning Meets Combinatorial Algorithms at NeurIPS2020*, 2020. URL <https://openreview.net/forum?id=IVc9hqqibyB>.
- Smith-Miles, K. and Bowly, S. Generating new test instances by evolving in instance space. *Computers & Operations Research*, 63:102–113, 2015.
- Tarjan, R. E. and Trojanowski, A. E. Finding a maximum independent set. *SIAM Journal on Computing*, 6(3):537–546, 1977.
- Vander Wiel, R. J. and Sahinidis, N. V. Heuristic bounds and test problem generation for the time-dependent traveling salesman problem. *Transportation Science*, 29(2):167–183, 1995.
- Wang, H. et al. Dig-milp: A deep instance generator for mixed-integer linear programming with feasibility guarantee. *arXiv preprint arXiv:2310.13261*, 2023.
- West, D. B. *Introduction to Graph Theory*. Prentice Hall, 2001.
- Wolsey, L. A. *Integer Programming*. John Wiley & Sons, 2 edition, 2020. ISBN 978-1-119-60653-6.
- Yang, T., Ye, H., and Xu, H. Learning to generate scalable milp instances. In *Proceedings of the Genetic and Evolutionary Computation Conference Companion*, 2024a.
- Yang, T., Ye, H., Xu, H., and Wang, H. MIPGen: Learning to Generate Scalable MIP Instances. In *Proceedings of the Twelfth International Conference on Learning Representations (ICLR 2024)*, April 2024b. URL <https://openreview.net/forum?id=YhwDw31DGI>. Under review at ICLR 2024.
- Zeng, H. et al. Effective generation of feasible solutions for integer programming via guided diffusion. In *Proceedings of the 30th ACM SIGKDD Conference on Knowledge Discovery and Data Mining*, 2024.
- Zhang, J., Liu, C., Li, X., Zhen, H.-L., Yuan, M., Li, Y., and Yan, J. A survey for solving mixed integer programming via machine learning. *Neurocomputing*, 519:205–217, 2023.
- Zhang, Y. et al. Milp-fbgen: Lp/milp instance generation with feasibility/boundedness. In *Forty-first International Conference on Machine Learning*, 2024.

A. Datasets

A.1. Ecole Synthesized Instances

To facilitate various experiments, including model training and evaluation across different metrics, 4 synthetic datasets of MILP instances was generated. This process utilized the **Ecole** library (Prouvost et al., 2020), a platform designed for machine learning research in combinatorial optimization.

Parameter Randomization: Parameters like the number of constraints, variables, and density are randomly sampled for each instance within the ranges specified in the configuration file. This ensures diversity in the generated dataset. The details of synthesizing parameters are in Table 10.

Table 10. Parameter Settings for MILP Instance Synthesis by Problem Type

Problem Type	Parameter	Value / Range
Set Cover (SC)	Constraints Range	[200, 800]
	Variables Range	[400, 1600]
	Density Range	[0.05, 0.2]
Capacitated Facility Location (CFL)*	Ratio (Facilities/Customers)	0.5
	Constraints Range	[50, 150]
	Variables Range	[500, 5000]
	Density Range	[0.01, 0.3]
Combinatorial Auction (CA)**	Number of Items (n_items)	Auto-calculated (null)
	Value Range (min/max)	[1, 100]
	Constraints Range	[50, 200]
	Variables Range	[80, 600]
	Density Range	[0.02, 0.1]
Independent Set (IS)***	Variables (Nodes) Range	[480, 520]
	Density (Edge Prob.) Range	[0.01, 0.015]
	Constraints Range	N/A (Derived)

*For CFL, the input ‘constraints’ and ‘variables’ ranges influence the number of customers and facilities, which in turn determine the actual model size. The ‘density’ range specified might not be directly used by the ‘ecole’ generator for CFL.

**For CA, the input ‘constraints’, ‘variables’, and ‘density’ ranges influence the number of bids and potentially items (if ‘n_items’ is null), which determine the actual model size.

***For IS, the ‘variables’ range directly corresponds to the number of nodes. The ‘constraints’ range is implicitly determined by the number of nodes and the edge probability (density) and is not directly set via ‘min/max_constraints’ in the config.

A.2. Compatibility Testing with Public Datasets (NIPS ML4CO)

In addition to utilizing the synthetically generated dataset described above, the compatibility and robustness of the various analysis pipelines and tools developed (e.g., for feature extraction, solver log parsing, model evaluation) were verified using publicly available MILP benchmark instances. Specifically, datasets from the **ML4CO Competition** (Gasse et al., 2022) were employed for testing purposes. Successfully processing and running analyses on these standard benchmarks demonstrated the broader applicability and compatibility of the developed experimental framework beyond the specific synthetically generated instances. More results are in Appendix L.3

B. More Related Work

The generation of high-quality MILP instances is crucial for developing, testing, and tuning both traditional solvers and modern ML approaches for combinatorial optimization. However, the scarcity of diverse, representative real-world instances, often due to proprietary constraints or collection difficulties, presents a significant bottleneck. This has spurred research into synthetic instance generation techniques. Recently, deep learning (DL) has emerged as a promising direction for MILP instance generation, aiming to automatically learn complex data distributions and structural features from existing instances without requiring explicit, expert-designed formulations. Several DL-based frameworks have been proposed:

VAE-based Approaches: G2MILP (Geng et al., 2023) introduced the first DL-based framework, using a masked Variational Autoencoder (VAE) paradigm. It iteratively corrupts and replaces constraint nodes in the bipartite graph representation.

While capable of generating instances structurally similar to the training data, G2MILP does not explicitly guarantee the feasibility or boundedness of the generated instances, potentially leading to unusable samples for certain downstream tasks. DIG-MILP (Wang et al., 2023), also VAE-based, addresses the feasibility and boundedness guarantee by leveraging MILP duality theories and sampling from a space including feasible solutions for both primal and dual formats. However, this can come at the cost of structural similarity compared to the original data. ACM-MILP (Guo et al., 2024) refines the VAE approach by incorporating adaptive constraint modification. It uses probability estimation in the latent space to select instance-specific constraints for modification, preserving core characteristics. It also groups strongly related constraints via community detection for collective modification, aiming to maintain constraint interrelations and improve hardness preservation.

Diffusion-based Approaches: Recognizing the power of diffusion models in generation tasks, MILP-FBGen (Zhang et al., 2024) proposed a diffusion-based framework. It uses a structure-preserving module to modify constraint/variable vectors and a feasibility/boundedness-constrained sampling module for the right-hand side and objective coefficients, aiming to ensure both structural similarity and feasibility/boundedness. Another diffusion-based approach focuses specifically on generating *feasible solutions* (rather than full instances) using guided diffusion. It employs contrastive learning to embed instances and solutions and uses a diffusion model conditioned on instance embeddings to generate solution embeddings, guided by constraints and objectives during sampling.

Structure-Focused Approaches: Some recent works explicitly target specific structural properties. MILP-StuDio (Liu et al., 2024) focuses on preserving and manipulating *block structures* commonly found in CCMs of real-world MILPs. It decomposes instances into block units, builds a library of these units, and uses operators (reduction, mix-up, expansion) to construct new, potentially scalable instances while maintaining structural integrity and properties like hardness and feasibility. MILPGen (Yang et al., 2024b) also aims at scalability, using node splitting/merging on the bipartite graph representation to decompose instances into tree structures, which are then concatenated to build larger problems.

These learning-based methods offer the potential to generate diverse and realistic MILP instances automatically, addressing the data scarcity issue. The generated instances have shown promise in downstream tasks like solver hyperparameter tuning, data augmentation for ML models predicting optimal values or guiding solvers, and potentially constructing harder benchmarks.

C. Parameter Summary

See the parameters of our methods in Table 11.

Table 11. Summary of Key Experimental Parameters.

Category	Parameter Name	Value	Description
Feasibility Ratio	Gurobi <code>time_limit</code>	300 s	Maximum Gurobi solve time per instance for feasibility/boundedness check.
	Feature Set	11 features	Set of graph-based structural features extracted (e.g., density, degree stats).
Structural Similarity	Comparison Metric	JSD-based	Jensen-Shannon Divergence ($1 - JSD / \log(2)$) averaged.
	Gurobi <code>time_limit</code>	300 s	Maximum Gurobi solve time per instance.
Branching Nodes	Gurobi <code>threads</code>	1	Threads per solve (to enhance determinism).
	Metric	Relative Error	$ \frac{\sum N_{gen}}{\sum N_{train}} - 1 \times 100\%$.
	Gurobi <code>time_limit</code>	3600 s	Maximum Gurobi solve time per instance.
Solving Time Gap	Gurobi <code>threads</code>	1	Threads per solve.
	Metric	Relative Difference	$ \frac{\text{mean } t_{gen}}{\text{mean } t_{train}} - 1 \times 100\%$.

Table 11. Summary of Key Experimental Parameters (Continued).

Category	Parameter Name	Value	Description
Hyperparameter Tuning	Tuning Framework	SMAC3	Automated algorithm configuration tool used.
	n_trials	50	SMAC3 evaluation budget.
	Objective	Mean Solve Time	Minimize mean wall-clock time on the tuning set.
	Gurobi time_limit	60 s	Gurobi time limit per solve during tuning/evaluation.
	Gurobi threads	1	Gurobi threads per solve during tuning/evaluation.
	Tuned Parameters	Gurobi Controls	8 parameters including Heuristics, MIPFocus, etc.
Initial Basis Prediction	<i>GNN Model Parameters</i>		
	num_layers	3	Number of GNN message passing layers.
	hidden_dim	128	Dimensionality of hidden layers in the GNN.
	dropout	0.1	Dropout rate used during training.
	<i>GNN Training Parameters</i>		
	Loss Function	Weighted CE	Weighted Cross-Entropy + Label Smoothing (0.1).
	<i>Evaluation Parameters</i>		
Gurobi time_limit	600 s	Gurobi time limit per solve during evaluation.	
Gurobi threads	1	Gurobi threads per solve during evaluation.	
	Basis Repair Threshold	1e-12	Pivot threshold for basis repair stability check.
Solver-Internal Features	<i>Data Generation Phase</i>		
	Gurobi time_limit	100 s	Gurobi time limit for log generation.
	<i>Comparison Phase</i>		
	Root Gap Metric	1-Wasserstein	Metric to compare scalar distributions.
	Cut Plane Metric	PCA + 1-W.	Method for comparing high-dim cut vectors.
	PCA Components	3	Number of components retained for cut analysis.
	PCA Scaling	Standard	Data scaling method (Z-score) before PCA.

D. Experiment Environment

All experiments were conducted on a Linux-based system equipped with an AMD EPYC 9754 128-Core Processor with a typical operating frequency around 3.1 GHz and supports 256 threads (128 cores with 2 threads per core). The system has 256 MiB of L3 cache and 251 GiB of system RAM.

For GPU-accelerated computations, a NVIDIA GeForce RTX 3090 graphics card with 24 GiB of VRAM was utilized. The NVIDIA driver version was 535.171.04, supporting CUDA up to version 12.2. The CUDA Toolkit version used for development and compilation was 11.8 (V11.8.89).

The operating system was Ubuntu 20.04.6 LTS. Key software includes Python 3.8.20, Gurobi Optimizer version 11.0.1.

E. More Preliminaries

Simplex Method Basics The **Simplex Method** (Dantzig, 1963) is an algorithm primarily designed for solving Linear Programming (LP) problems, such as the LP relaxation defined above. While it can handle various forms, it often operates by converting the problem to a standard form like $\min\{\mathbf{c}'^\top \mathbf{y} \mid \mathbf{A}'\mathbf{y} = \mathbf{b}', \mathbf{y} \geq 0\}$ (where \mathbf{y} might include original and slack/surplus variables). It explores the vertices (Basic Feasible Solutions, BFS) of the feasible polyhedron $\mathcal{P}' = \{\mathbf{y} \mid \mathbf{A}'\mathbf{y} = \mathbf{b}', \mathbf{y} \geq 0\}$. It iteratively moves between adjacent BFS by exchanging one variable in the current basis (a set of variables determining the BFS) with a non-basic variable, guided by criteria like reduced costs to ensure monotonic improvement of the objective function value, until an optimal BFS is found or unboundedness is detected.

Heuristics Within MILP solvers, **heuristics** (Berthold, 2012) are algorithms designed to rapidly find a feasible integer solution $\hat{\mathbf{x}} \in \mathcal{F}_{MILP} = \{\mathbf{x} \mid \mathbf{A}\mathbf{x} \leq \mathbf{b}, x_i \in \mathbb{Z} \forall i \in \mathcal{I}\}$, whose objective value $\tilde{\mathbf{c}}^\top \hat{\mathbf{x}}$ is hopefully close to the true optimum z_{MILP} . They do not guarantee optimality. Their main purpose is to quickly establish strong primal bounds (updating the incumbent $z_{incumbent} = \min(z_{incumbent}, \tilde{\mathbf{c}}^\top \hat{\mathbf{x}})$). In branch-and-bound, these incumbents enable pruning of search nodes j where the local lower bound $z_{bound}^{(j)}$ satisfies $z_{bound}^{(j)} \geq z_{incumbent}$.

Cutting Planes (Cuts) **Cutting planes** (Conforti et al., 2014) are linear inequalities, $\alpha^T \mathbf{x} \leq \beta$, that are valid for all feasible integer solutions, i.e., they hold for all $\mathbf{x} \in \text{Conv}(\mathcal{F}_{MILP})$ where $\mathcal{F}_{MILP} = \{\mathbf{x} \mid \mathbf{A}\mathbf{x} \leq \mathbf{b}, x_i \in \mathbb{Z} \forall i \in \mathcal{I}\}$. However, they are chosen such that they are violated by the optimal solution \mathbf{x}_{LP}^* of the current LP relaxation (i.e., $\alpha^T \mathbf{x}_{LP}^* > \beta$). Adding such cuts \mathcal{C} to the LP relaxation feasible set $\mathcal{P} = \{\mathbf{x} \mid \mathbf{A}\mathbf{x} \leq \mathbf{b}\}$ yields a tighter relaxation $\mathcal{P}' = \mathcal{P} \cap \{\mathbf{x} \mid \alpha^T \mathbf{x} \leq \beta \text{ for all } \alpha^T \mathbf{x} \leq \beta \in \mathcal{C}\}$. The goal is to improve the lower bound derived from the relaxation, $\min_{\mathbf{x} \in \mathcal{P}'} \tilde{\mathbf{c}}^\top \mathbf{x} \geq z_{LP}$, thereby bringing it closer to the true MILP optimum z_{MILP} and potentially reducing the search space.

F. Feasibility

Below is the result of feasibility test.

Table 12. Feasibility and Boundedness Ratios Across All Problem Types. Each configuration was tested on 1000 instances.

Problem	Model	Ratio (η)	Feasible (%)
Independent Set	Original Set	N/A	100.00
	G2MILP	0.01	100.00
		0.05	100.00
		0.10	93.40
	ACM-MILP	0.05	100.00
		0.10	100.00
0.20		100.00	
Combinatorial Auction	Original Set	N/A	100.00
	ACM-MILP	0.05	100.00
		0.10	100.00
		0.20	100.00
	DIG-MILP	0.01	100.00
		0.05	100.00
0.10		100.00	
Set Cover	Original Set	N/A	100.00
	G2MILP	0.01	100.00
		0.05	100.00
		0.10	100.00

G. Structural Similarity

The experiment’s objective is to quantitatively compare the structural similarity between two sets of MILP instances. This is achieved by extracting graph-based structural features from each instance and then calculating the Jensen-Shannon Divergence (JSD) to measure the difference between the feature distributions of the two sets.

G.1. Methodology

1. Feature Extraction: Each MILP instance is converted into a bipartite graph. From this graph, a vector of structural features is extracted, capturing characteristics related to matrix sparsity, variable and constraint connectivity, coefficient statistics, and other graph-theoretic properties. This process is computationally parallelized for efficiency. The specific features are grouped into two categories and detailed in Table 13.

Table 13. Structural Features Used for Similarity Analysis

Category	Feature	Metric(s)	Description
Basic Graph Features	Coefficient Density	<code>coef_dens</code>	Reflects the sparsity of the constraint matrix.
	Variable Node Degree	<code>var_degree_mean/std</code>	Describes the occurrence patterns of variables in constraints.
	Constraint Node Degree	<code>cons_degree_mean/std</code>	Reflects the number of variables involved in each constraint.
	Coefficient Statistics	<code>lhs/rhs_mean/std</code>	Captures the numerical distribution of constraint terms.
Advanced Topological	Clustering Coefficient	<code>clustering</code>	Measures the local connection density between variables.
	Modularity	<code>modularity</code>	Assesses the degree of modularity in the problem structure.

2. Per-Feature Similarity: For each feature, the Jensen-Shannon Divergence is used to compare its distribution across the two sets of instances. This divergence value is then normalized to a similarity score ranging from 0 (maximal divergence) to 1 (identical distributions).

3. Overall Similarity Score: A final, overall similarity score is calculated by taking the arithmetic mean of all the individual feature similarity scores. This single metric represents the aggregate structural similarity between the two instance sets.

H. Solving Time Gap

This experiment assesses the similarity in computational hardness between a ‘training’ set and a ‘generated’ set of MILP instances. The metric is the relative percentage difference in their average solve times using the Gurobi optimizer.

Methodology: Each instance from both sets is solved under identical Gurobi configurations to ensure a fair comparison. The key parameters are:

- **Time Limit:** 300 seconds per instance.
- **Threads:** 256 per instance.

The average solve time is computed for each set. The final metric is calculated using the formula:

$$\text{Relative Time Gap} = \frac{|\text{generated_mean_time} - \text{training_mean_time}|}{\max(\text{training_mean_time}, 10^{-10})} \times 100\%$$

A lower percentage signifies a greater similarity in computational hardness between the two instance sets.

H.1. Results

The results are in Table 14. We have omitted the G2MILP-generated Independent Set (IS) instances from this presentation. The rationale for this decision lies in the substantial surge in their computational complexity compared to the baseline

instances, leading to a prohibitive increase in solution times by a factor of several thousands.

Table 14. Solving Time Gap Comparison. The table shows the percentage difference in average solving time between instances generated by different sources (with varying mask ratios η) and the original training set instances. **Original** refers to the baseline training set. G2MILP instances for IS reached the 300s time limit.

Dataset	Source	η	Avg Time (s)	Solving Time Gap (%)
SC	Original	—	0.2644	—
	G2MILP	0.10	0.3002	13.54
		0.05	0.2945	11.38
		0.01	0.3237	22.43
CA	Original	—	0.1020	—
	ACM-MILP	0.20	2.6449	2493.04
		0.10	3.1654	3003.33
		0.05	3.4461	3278.53
	DIG-MILP	0.10	0.1312	28.63
		0.05	0.1225	20.10
		0.01	0.1237	21.27
	IS	Original	—	0.3374
ACM-MILP		0.20	0.1722	48.96
		0.10	0.1774	47.42
		0.05	0.1788	47.01
G2MILP		0.10	300.00	88815.23
		0.05	300.00	88815.23
		0.01	300.00	88815.23

I. Hyperparameter Tuning for Gurobi

The objective of this project is to automatically tune a key set of Gurobi solver hyperparameters using the SMAC3 framework. The goal is to find a parameter configuration that **minimizes the average wall-clock solve time** for a specific collection of MILP instances, designated as the **tuning set**. Subsequently, the performance of this optimized configuration is compared against Gurobi’s default settings on a separate, unseen **test set** to evaluate its generalization capability.

I.1. Methodology

The process is divided into five phases to ensure robust optimization and an unbiased evaluation.

Phase 1: Inputs and Setup The process utilizes two independent sets of MILP instances: a **tuning set**, which is used to train the SMAC3 model and guide its search for optimal parameters, and a separate **test set**, which is held out exclusively for the final performance evaluation to ensure an objective assessment. The core tuning engine is **SMAC3**, which directly interfaces with the target solver, **Gurobi**.

Phase 2: Hyperparameter Space Definition We selected eight critical Gurobi hyperparameters for optimization. The parameter space includes one continuous parameter, `Heuristics`, defined on the range $[0.0, 1.0]$. The remaining seven parameters are categorical: `MIPFocus` $\{0, 1, 2, 3\}$, `VarBranch` $\{-1, 0, 1, 2, 3\}$, `BranchDir` $\{-1, 0, 1\}$, `Presolve` $\{-1, 0, 1, 2\}$, `PrePasses` $\{-1, \dots, 20\}$, `Cuts` $\{-1, 0, 1, 2, 3\}$, and `Method` $\{-1, \dots, 5\}$.

Phase 3: Automated Tuning with SMAC3 SMAC3 performs an iterative optimization over a budget of **50 trials**. Each trial begins with SMAC3 suggesting a new hyperparameter configuration from its internal model. Gurobi then uses this configuration to solve all instances in the **tuning set**, with each solve constrained to a **60-second time limit** and using **256 threads**. The resulting **average solve time** across the set is calculated and returned to SMAC3 as a cost metric. This

feedback allows SMAC3 to update its model and inform its choice for the next trial. Upon completion, SMAC3 reports the **best configuration** found, which is the one that yielded the lowest average solve time.

Phase 4: Performance Evaluation on the Test Set To assess generalization, we compare the **best configuration** found by SMAC3 against Gurobi’s **default configuration** on the independent **test set**. Both configurations are run under identical computational conditions (60-second time limit, 256 threads) to ensure a fair and direct comparison of their performance.

Phase 5: Outputs and Analysis The final outputs synthesize the results into two key components. The primary metric is a comparison of the average solve times on the test set for the best versus default configurations, often expressed as a percentage improvement. The analysis also provides the **best configuration** itself, detailing the specific values for the eight optimized hyperparameters that yielded the top performance.

Table 15 shows the best Gurobi hyperparameter values found by SMAC3 for each experiment. The default Gurobi parameter values are: `Heuristics=0.05`, `MIPFocus=0`, `VarBranch=-1`, `BranchDir=0`, `Presolve=-1`, `PrePasses=-1`, `Cuts=-1`, `Method=-1`.

Table 15. Best Gurobi hyperparameter values found for each experiment. Column Abbreviations: `Heur.:` Heuristics, `Focus:` MIPFocus, `VarBr.:` VarBranch, `BrDir.:` BranchDir, `Pres.:` Presolve, `PreP.:` PrePasses, `Cuts:` Cuts, `Meth.:` Method.

Experiment Name	Heur.	Focus	VarBr.	BrDir.	Pres.	PreP.	Cuts	Meth.
acmmilp_mis_0.1	0.189	2	1	-1	-1	10	0	5
acmmilp_mis_0.2	0.474	0	1	0	-1	17	1	2
acmmilp_mis_0.05	0.500	0	-1	-1	-1	-1	-1	-1
ca	0.186	1	1	1	0	1	-1	4
digmilp_ca_0.1	0.186	1	1	1	0	1	-1	4
digmilp_ca_0.05	0.186	1	1	1	0	1	-1	4
digmilp_ca_0.01	0.186	1	1	1	0	1	-1	4
mis	0.498	0	1	-1	1	-1	1	3
setcover	0.189	2	1	-1	-1	10	0	5
g2milp_setcover_0.01	0.189	2	1	-1	-1	10	0	5
g2milp_setcover_0.05	0.189	2	1	-1	-1	10	0	5

J. Initial Basis Prediction

Following (Fan et al., 2023), this experiment utilizes Graph Neural Networks (GNNs) to predict a high-quality initial basis for the LP relaxation of MILP instances. The objective is to train a GNN on ****an augmented dataset (combining original and generated instances)**** and evaluate whether its predicted basis accelerates Gurobi compared to default initialization. Performance is measured by Gurobi runtime, node count, and iteration count on an unseen test set.

J.1. Methodology & Operations

The methodology employs a six-phase approach: transforming MILP instances into graph representations, feature extraction, model training, and performance evaluation. This process ensures robust basis prediction while maintaining numerical stability.

Phase 1: Problem Description and Data Representation MILP instances are defined by constraint matrix A , RHS vector b , objective c , and variable bounds l, u . The prediction task identifies an optimal initial basis, defined by sets B and N (where $B \cup N = \{1, \dots, n\}$), ensuring the basis matrix is non-singular.

Instances are transformed into bipartite graphs $G = (V, E)$. V contains variable and constraint nodes; E represents structural relationships where edge exists if $(i, j) \in E$, weighted by A_{ij} .

Phase 2: Feature Engineering Node representations capture both local structure and global characteristics. Variable node features (8 dimensions) include: objective coefficient c_i , variable density d_i , and similarity to slack bounds (e.g., $u_i - l_i$). Bounds are

encoded via numerical values and binary flags (finite vs. infinite).

Constraint node features (8 dimensions) include: similarity to objective, constraint density, and similarities to variable bounds. Continuous features (excluding binary flags) undergo z-score standardization for training stability.

Phase 3: Graph Neural Network Model The hierarchical GNN architecture processes the bipartite structure. An initial MLP projects 8-dimensional inputs to a 128-dimensional hidden space. The core comprises `BipartiteMessagePassing` layers with residual connections to aggregate neighborhood information.

Separate MLP heads output 3-dimensional logits for variables and constraints, corresponding to basis states: `NonbasicAtLower`, `Basic`, and `NonbasicAtUpper`. Knowledge masking enforces physical constraints by blocking impossible states based on bounds. Final probabilities are obtained via softmax on masked logits, utilizing dropout (0.1) for regularization.

Phase 4: Model Training A `GNNTrainer` trains the model using a composite dataset where generated instances are added to the original baseline. The training runs for up to 800 epochs with a batch size of 32. The loss function uses label smoothing (0.1) to improve generalization and dynamic class weights to handle class imbalance. Optimization employs Adam (learning rate $1e-3$) with L2 weight decay ($1e-4$). Early stopping terminates training if validation loss stagnates for 50 epochs, preserving the best-performing weights.

Phase 5: Initial Basis Generation and Repair GNN predictions are converted into a numerically stable basis. Candidates are selected based on the highest predicted "Basic" probabilities. To ensure non-singularity, a repair process performs LU decomposition on the candidate matrix, iteratively replacing unstable columns. Finally, nonbasic variables are assigned states (`NonbasicAtLower` or `NonbasicAtUpper`) according to their predicted probability distributions.

Phase 6: Performance Evaluation The evaluation compares the GNN-predicted basis against Gurobi's default initialization on an independent test set. Metrics include runtime, node count, and iteration count, providing a comprehensive assessment of the algorithmic efficiency gains achieved by the learned initialization.

K. Solver-Internal Features

This experiment analyzes the behavioral patterns of the Gurobi solver to compare original and generated sets of MILP instances. The methodology involves a two-phase process: first, we gather detailed performance metrics by solving each instance, and second, we apply statistical techniques to quantify the similarity between the instance sets based on the solver's behavior.

Methodology

Phase 1: Data Generation and Metric Extraction In the first phase, we solve every MILP instance from both the original and generated collections using Gurobi under identical, standardized settings. This controlled environment ensures that any observed differences in performance are attributable to the instances themselves, not the solver's configuration. We enable detailed logging to capture a comprehensive record of the solver's internal operations.

From these logs, we systematically parse and extract key operational metrics. These metrics include the **duality gap at the root node**, which indicates initial problem difficulty; the **success counts of various heuristics**, which measure the effectiveness of the solver's solution-finding strategies; and the **usage frequency of different cut plane types** (e.g., Gomory, Cover, MIR), which reveals the solver's approach to tightening the LP relaxation. This process transforms the raw log files into structured data, ready for quantitative analysis.

Phase 2: Comparative Statistical Analysis The second phase quantifies the similarity between the original and generated instance sets by comparing the distributions of the metrics collected in Phase 1. We primarily use the **1-Wasserstein distance** as a robust measure of distributional difference—a smaller distance implies greater similarity.

For one-dimensional metrics like the root node gap and heuristic success counts, we directly compare their distributions. For the multi-dimensional cut plane data, we first normalize the usage counts for each instance into proportions. We then apply **Principal Component Analysis (PCA)** to reduce the dimensionality of this data, focusing the comparison on the most significant patterns of solver behavior. The Wasserstein distance is then used to compare the instance sets along these

principal components. The final output consists of these distance values, which serve as a quantitative score of behavioral similarity between the two datasets.

Table 16. Root Node Gap Statistics Comparison (Dataset Halves)

Statistic	part1	part2
count	500	500
mean	3.4637	3.4194
std	1.4386	1.4514
min	0.9722	1.0417
25%	2.2222	2.4094
50%	3.4483	3.2076
75%	4.6289	4.5045
max	6.1364	6.5909
W-Dist.	0.1884	0.1884

Table 17. Heuristic Success Count Statistics Comparison (Dataset Halves)

Statistic	part1	part2
count	500	500
mean	6.0380	6.0400
std	1.7879	1.9541
min	2.0000	2.0000
25%	5.0000	4.0000
50%	6.0000	6.0000
75%	7.0000	7.0000
max	11.0000	11.0000
W-Dist.	0.1300	0.1300

K.1. Visualization

Here are some figures 3 4,5,6 showing the results of solver internal features comparison.

K.2. Efficiency Test on Super Hard Instances

K.2.1. EXPERIMENTAL OBJECTIVE

To validate the practical feasibility and robustness of our solver-internal feature analysis method, we designed an efficiency test. The core goal of this experiment is to demonstrate that even under strict computational constraints (i.e., tight time limits) and when facing a well-known set of hard instances, our method can still stably and efficiently extract meaningful feature distributions. This supports our key hypothesis that obtaining such deep behavioral features does not require solving instances to optimality, thereby making the evaluation both low-cost and highly efficient.

K.2.2. EXPERIMENTAL METHODOLOGY

Dataset Selection: We used the `item_placement` dataset from the ML4CO competition, which is recognized for its high solving difficulty. A total of 1000 instances were selected for testing.

Computational Budget Constraint: To simulate scenarios with limited computational resources, we imposed a strict time limit of **120 seconds** for the Gurobi solver on each instance.

Validation Method: We employed a split-half validation approach to evaluate the stability of the extracted features:

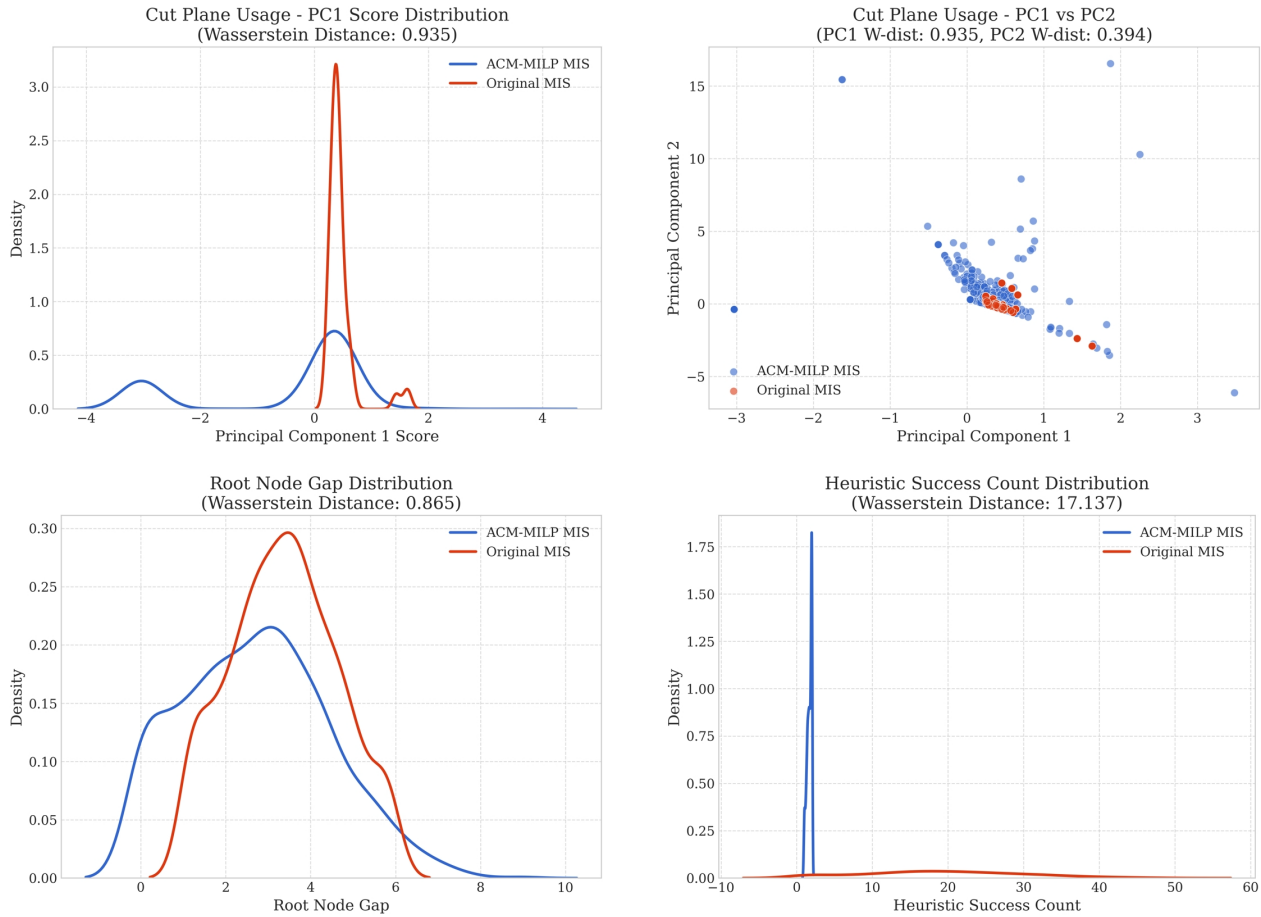


Figure 3. ACM-MILP IS at $\eta = 0.1$ compared with Original Dataset

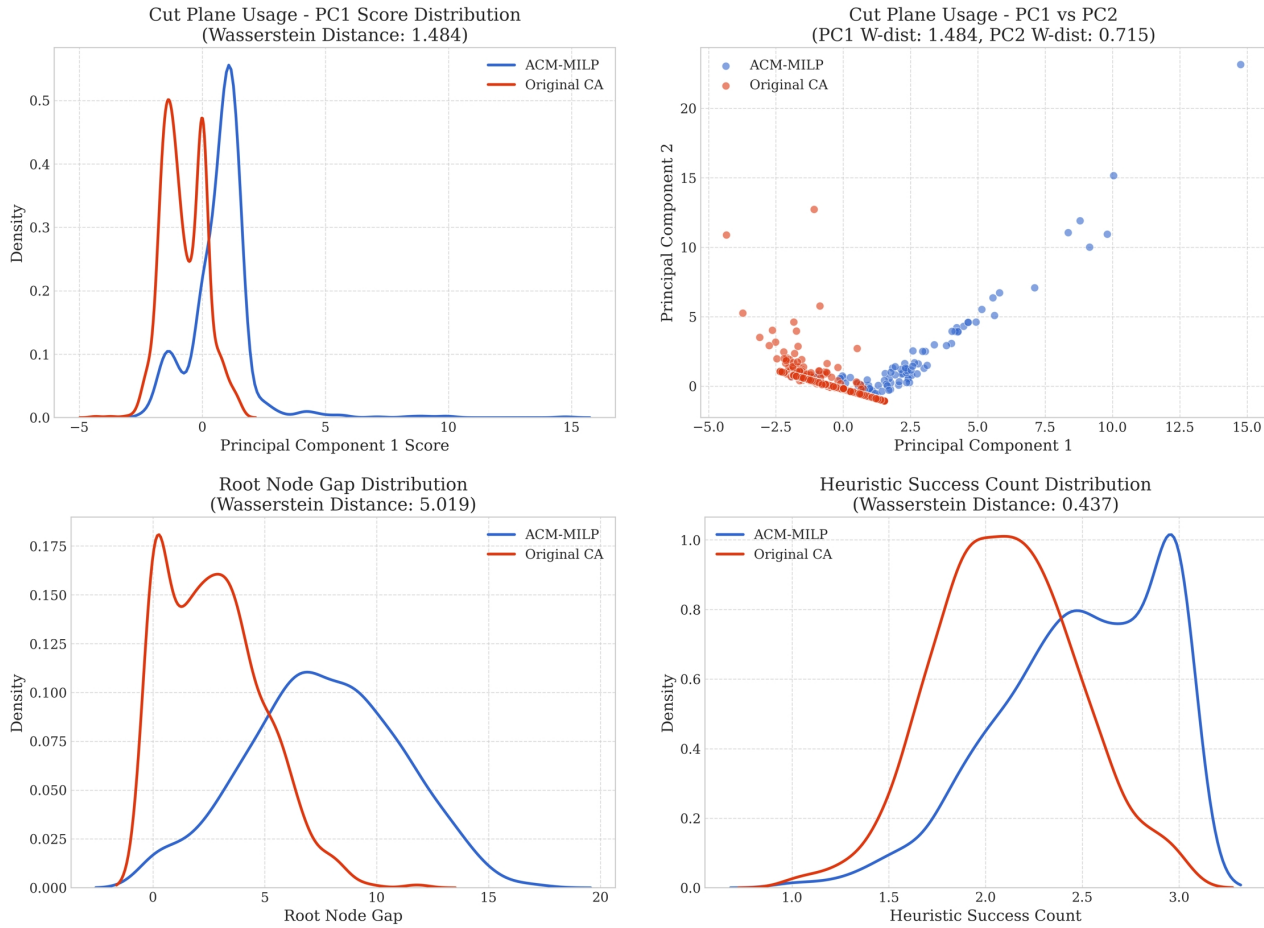


Figure 4. ACM-MILP CA at $\eta = 0.1$ compared with Original Dataset

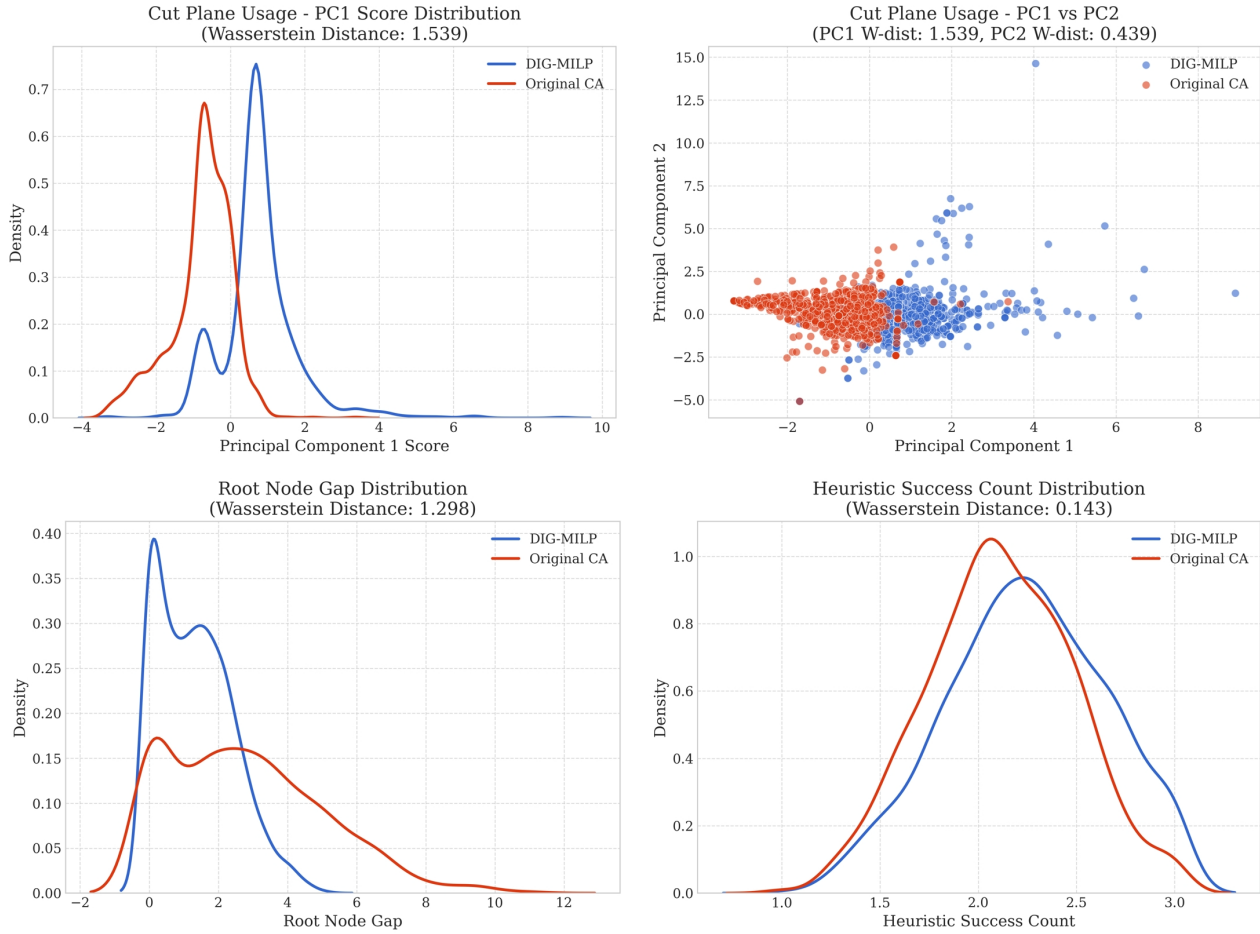


Figure 5. DIG-MILP CA at $\eta = 0.1$ compared with Original Dataset

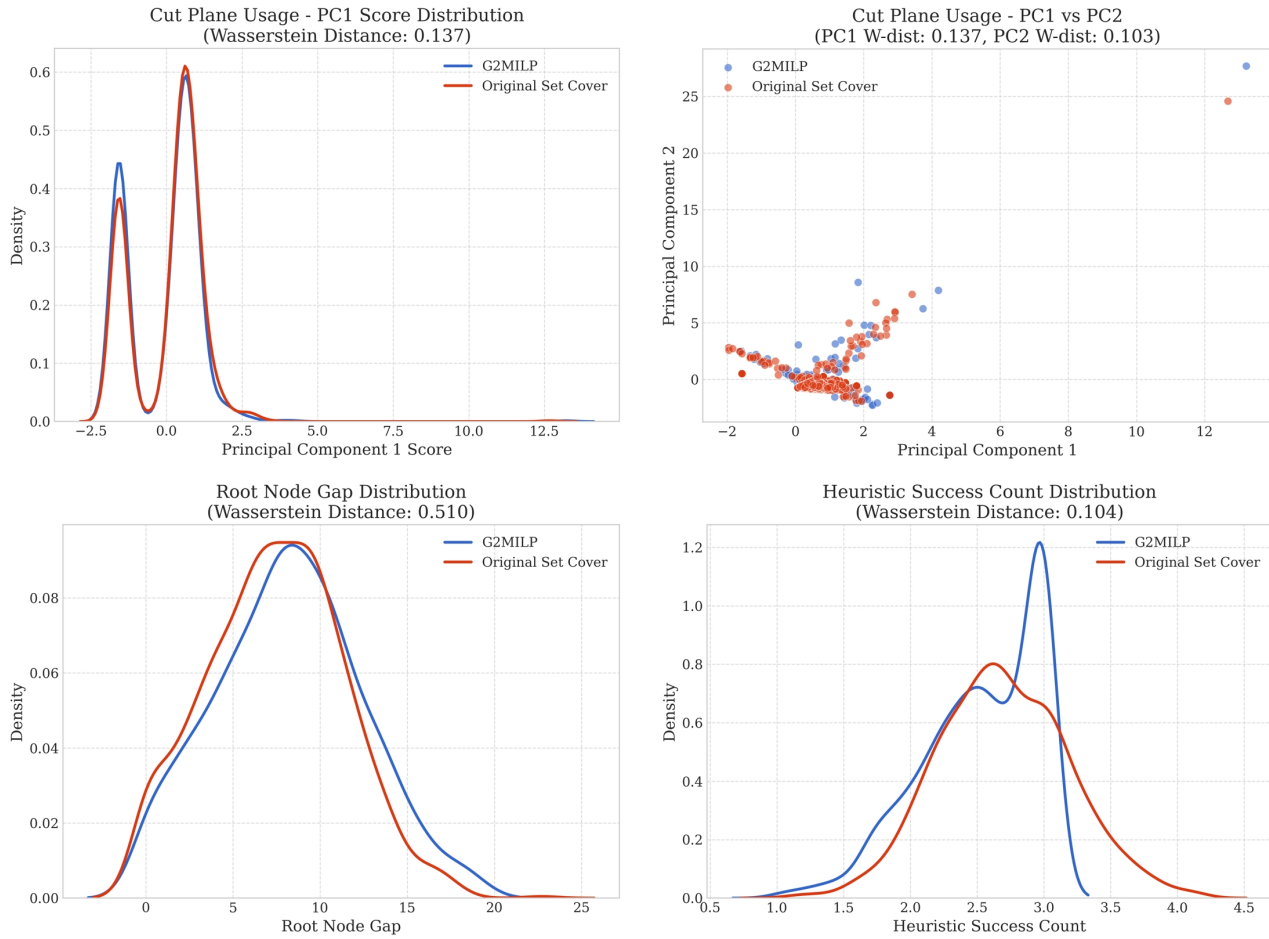


Figure 6. G2MILP SC at $\eta = 0.1$ compared with Original Dataset

Table 18. Cut Plane Usage PCA 1-Wasserstein Distances (Dataset Halves)

Principal Component	W-Dist.
PC1	0.2318
PC2	0.3295
PC3	0.2280

Table 19. Overall Gurobi Solver Metrics Across Datasets

Dataset	Avg. Root Gap (%)	Heuristic Successes
IS (Raw)	3.42	18883
Combinatorial Auction (Raw)	2.47	2115
Set Cover (Raw)	7.61	2702
ACM-MILP CA ($\eta = 0.1$)	7.49	2552
ACM-MILP IS ($\eta = 0.1$)	2.66	1746
DIG-MILP CA ($\eta = 0.05$)	1.09	2241
G2MILP SetCover ($\eta = 0.05$)	7.75	2600

- The 1000 solver logs were randomly divided into two halves, each containing 500 instances.
- We independently extracted solver-internal features from each half, including Root Node Gap, Heuristic Success Count, and Cut Plane Usage.
- We then computed and compared the distributional similarity of these features across the two halves. If the random subsets originating from the same underlying distribution exhibit highly similar feature distributions (i.e., low Wasserstein distance), it indicates strong stability and reliability of the feature-extraction method.

K.2.3. EXPERIMENTAL RESULTS

The split-half experiment clearly shows that even under strict time constraints, the distributions of solver-internal features extracted from the solving process remain highly stable. Key indicators and their 1-Wasserstein distances are summarized in Table 21.

K.2.4. CONCLUSION

This experiment strongly demonstrates the practical value of our framework:

- **High Efficiency and Low Cost:** The results confirm that a truncated solving process (120-second timeout) is sufficient to extract stable and representative solver-internal feature distributions. This substantially reduces the time and computational cost of evaluating large-scale or extremely hard instance sets.
- **Feature Stability:** The very small Wasserstein distances observed for Root Node Gap and Cut Plane Usage indicate that these early-stage solver behavior features are highly stable.

Table 20. Aggregated Cut Plane Counts (Sum over 1000 instances)

Dataset	Gomory	ZeroHalf	Clique	MIR	RLT	FlowCover	Cover	ModK	RelaxLift	InffProof	StrongCG	ImplBound
IS (Raw)	1305	61590	89	58	43763	0	0	0	0	0	0	0
Combinatorial Auction (Raw)	11183	7014	8941	98	81	0	3	24	0	0	6	0
Set Cover (Raw)	1350	3473	80	5601	240	0	0	8	0	0	0	1
ACM-MILP CA ($\eta = 0.1$)	6524	3132	26779	25	2	229	86	3	4	3	0	0
ACM-MILP IS ($\eta = 0.1$)	1087	34032	33	13	22932	0	0	1	0	0	0	0
DIG-MILP CA ($\eta = 0.05$)	6024	5629	462	531	114	0	14	34	0	1	14	0
G2MILP SetCover ($\eta = 0.05$)	1330	3228	31	5454	209	0	0	8	0	0	0	0

Table 21. W-1 distances of key solver-internal features across two random halves

Feature Dimension	W-1 Dist.	Remarks
Root Node Gap	0.7613	Mean difference only 0.04%; identical standard deviation
Heuristic Success Count	0.7320	Mean and standard deviation are very close
Cut Plane Usage		Compared on top 3 principal components after PCA
– PC1	0.0917	Extremely low distance indicates highly consistent cut-plane usage pattern
– PC2	0.0870	
– PC3	0.0904	

- **Practical Feasibility:** The success of this test shows that the GenBench-MILP framework is not only theoretically sound but also practically applicable for evaluating MILP instances that are difficult to solve to optimality within a reasonable time frame and that reflect real-world complexity.

K.3. Tests on Other Solvers

K.3.1. EXPERIMENTAL OBJECTIVE

To validate the generality of the GenBench-MILP framework and to investigate potential differences in solver-internal behavioral features, we applied our core solver-internal feature analysis method to two leading open-source solvers: **SCIP** and **HiGHS**. This experiment is designed to answer two key questions:

1. *Can our framework be flexibly adapted to solvers other than Gurobi?*
2. *Do different solvers exhibit varying stability in their internal behaviors when solving the same instance set?*

K.3.2. EXPERIMENTAL METHODOLOGY

We adopted the same split-half validation method used in the Gurobi experiments. Using the original Independent Set (IS) dataset, we randomly divided the instances into two subsets of 500 instances each. SCIP and HiGHS were then used to solve the two subsets separately, extracting three categories of solver-internal features: Root Node Gap, Heuristic Success, and Cut Plane Usage. Finally, we computed the 1-Wasserstein distance of these feature distributions between the two subsets to quantify the stability of each solver’s internal behavior. For a stable solver, the Wasserstein distance between random subsets originating from the same distribution should remain very small.

K.3.3. EXPERIMENTAL RESULTS AND ANALYSIS

Our results show that, while the framework can be successfully applied to all tested solvers, their internal feature stability varies substantially.

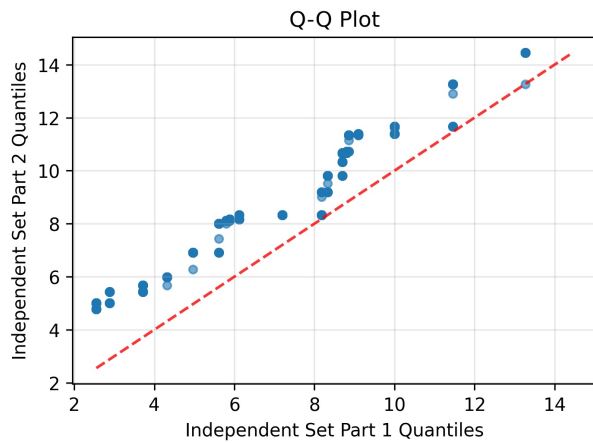
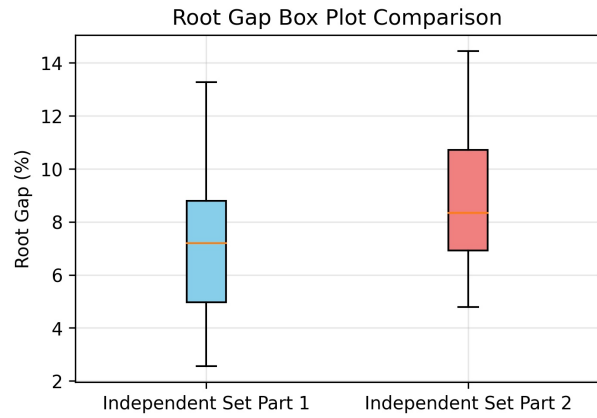
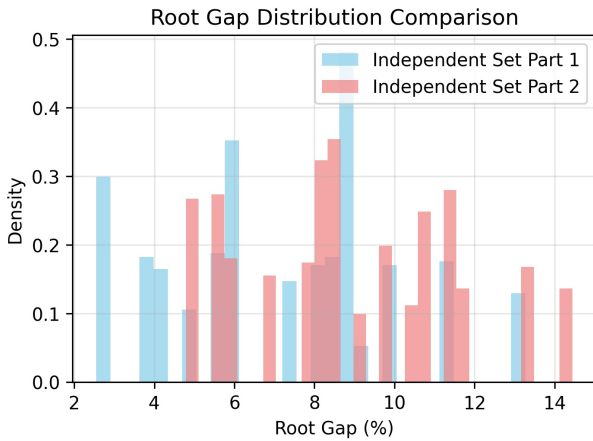
SCIP Solver Here are some figures 7, 8 and 9 showing the function of SCIP in split-half validation. For SCIP, the split-half experiment yields the following:

- **Root Node Gap:** The two subsets exhibit mean gaps of 7.13% and 8.88%, respectively. The Wasserstein distance is 1.753, which is much larger than the 0.1884 observed for Gurobi, indicating lower stability for SCIP in this metric.
- **Heuristic Success:** Principal Component Analysis (PCA) of six heuristic methods shows Wasserstein distances of PC1: 0.319, PC2: 0.426, and PC3: 0.778.
- **Cut Plane Usage:** PCA on four cut-plane types gives Wasserstein distances of PC1: 0.700, PC2: 0.298, and PC3: 0.241.

HiGHS Solver Here are some figures 10, 11 and 12 showing the function of HiGHS in split-half validation. For HiGHS, the differences are even more pronounced:

- **Root Node Gap:** The two subsets have mean gaps of 364.28% and 386.68%, respectively. The Wasserstein distance reaches 26.7297, indicating extremely unstable root-node relaxation behavior.

SCIP Root Gap Distribution Comparison



Statistical Summary:

Wasserstein Distance: 1.7532

Independent Set Part 1:

Mean: 7.13%
 Median: 7.20%
 Std: 2.82%

Independent Set Part 2:

Mean: 8.88%
 Median: 8.33%
 Std: 2.62%

Effect Size (Cohen's d): -0.645
 Interpretation: medium

Mann-Whitney U Test:
 p-value: 0.0000
 Significant: True

Figure 7. Comparison of Root Node Gap distributions for SCIP in split-half validation. The two distributions represent the two random halves of the instance set.

SCIP Cutting Planes PCA Comparison

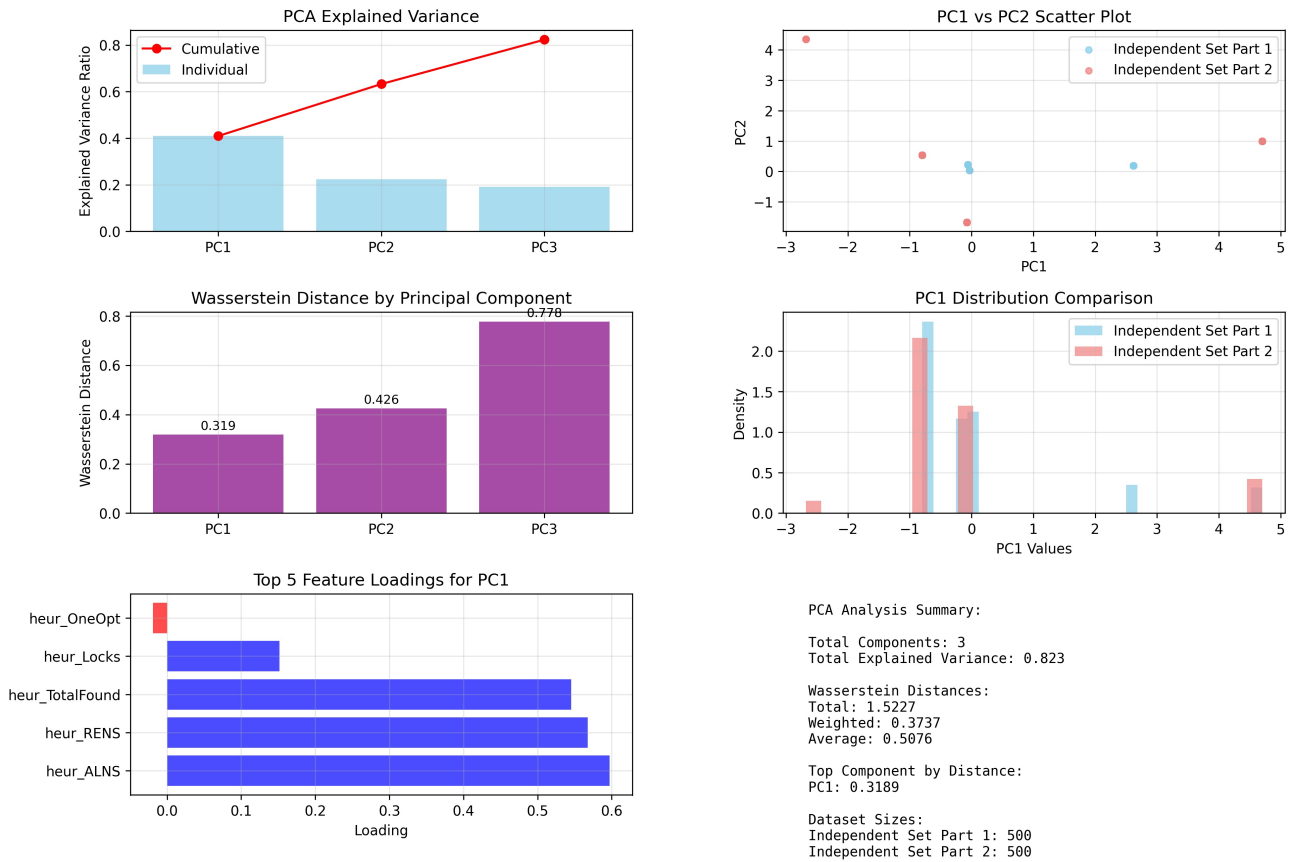


Figure 8. Comparison of Heuristic distributions for SCIP in split-half validation. The two distributions represent the two random halves of the instance set.

SCIP Cutting Planes PCA Comparison

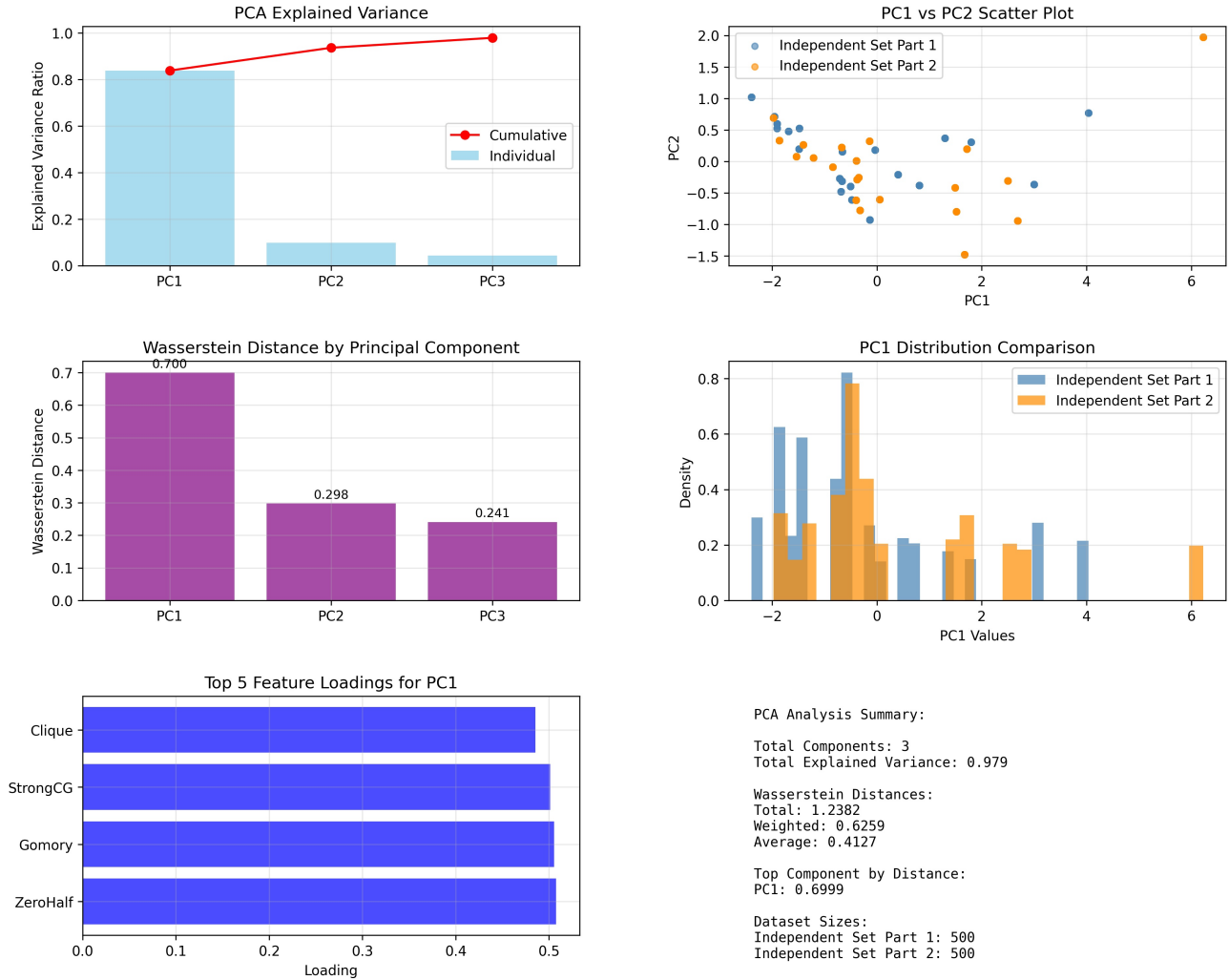


Figure 9. Comparison of cut plane distributions for SCIP in split-half validation. The two distributions represent the two random halves of the instance set.

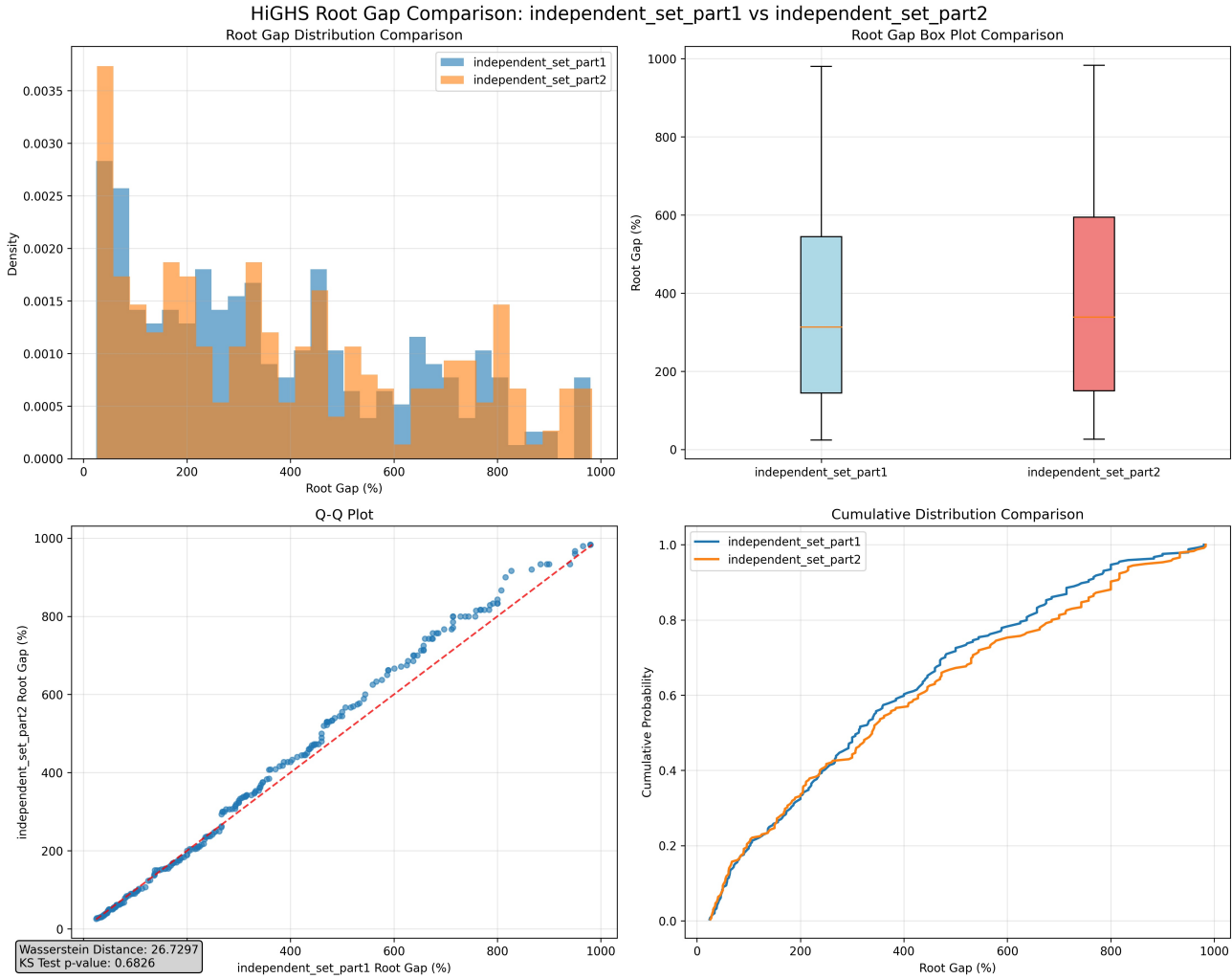


Figure 10. Comparison of root node gap distributions for HiGHS in split-half validation. The two distributions represent the two random halves of the instance set.

- **Heuristic Success:** PCA analysis of heuristic methods gives Wasserstein distances of PC1: 0.2368 and PC2: 0.1695, with a weighted average of 0.1530, reflecting good stability.
- **Cut Plane Usage:** HiGHS shows very consistent cut-plane usage. PCA reveals that the first principal component explains 100% of the variance, with a Wasserstein distance of only 0.0612, indicating highly stable cut-plane strategies.

K.3.4. CROSS-SOLVER COMPARISON

To facilitate comparison, Table 22 summarizes key 1-Wasserstein distances from the IS split-half validation for Gurobi, SCIP, and HiGHS.

Table 22. 1-Wasserstein distances across solvers on IS split-half validation

Feature Dimension	Gurobi (Baseline)	SCIP	HiGHS
Root Node Gap	0.1884	1.7530	26.7297
Heuristic (PC1)	0.1300	0.3190	0.2368
Cut Plane (PC1)	0.2318	0.7000	0.0612

PC1 Analysis (Wasserstein Distance: 0.2368)

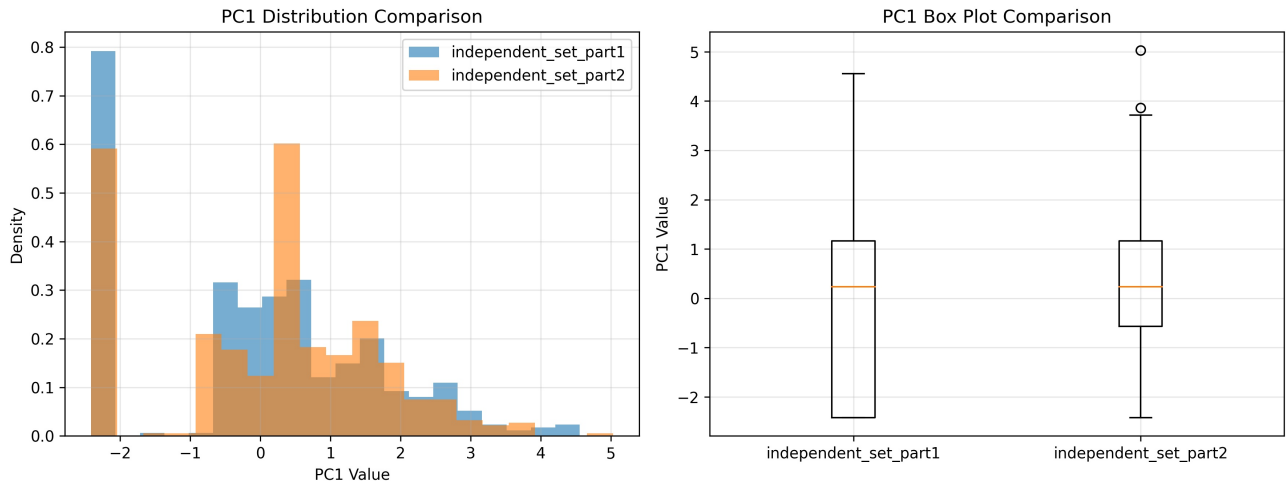


Figure 11. Comparison of heuristic distributions for HiGHS in split-half validation. The two distributions represent the two random halves of the instance set.

PC1 Analysis (Wasserstein Distance: 0.0612)

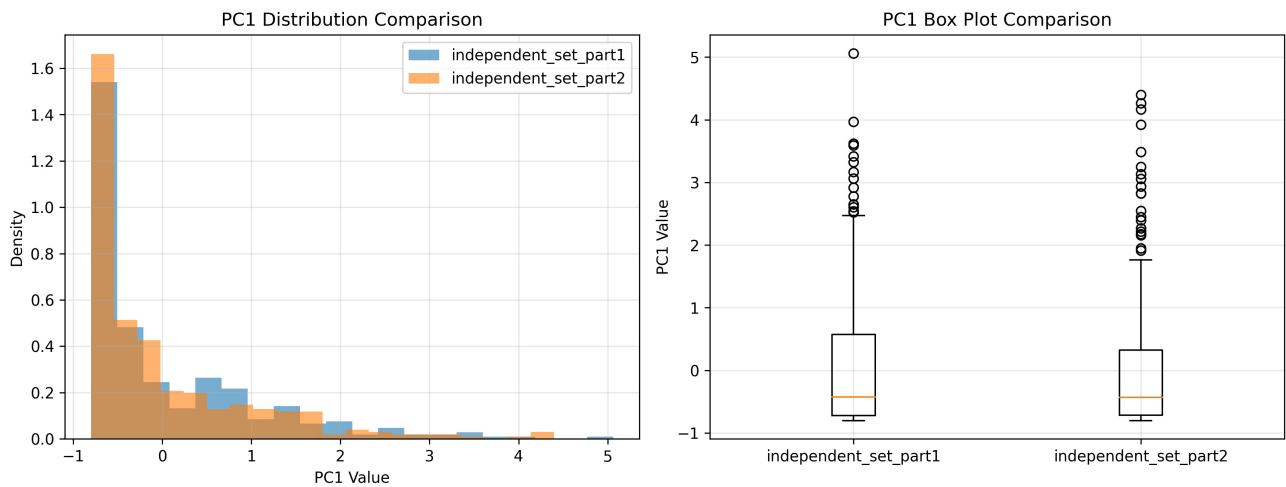


Figure 12. Comparison of cut plane distributions for HiGHS in split-half validation. The two distributions represent the two random halves of the instance set.

From the table we draw three key conclusions:

- **Framework Generality:** GenBench-MILP can be successfully applied to SCIP and HiGHS, confirming its potential as a general-purpose evaluation tool.
- **Stability Differences Across Solvers:** The most striking observation is the difference in Root Node Gap stability. Gurobi demonstrates exceptionally high stability, SCIP shows moderate instability, and HiGHS exhibits severe instability. This implies that solver strategies (e.g., preprocessing, initial LP relaxations) may have fundamentally different sensitivities to small instance perturbations.
- **Rationale for Choosing Gurobi as Baseline:** These findings strongly justify using Gurobi as the “expert evaluator” in our main study. Accurate and reliable instance-quality assessment demands a solver with highly stable internal behavior. Gurobi’s stability enables precise detection of subtle computational similarities between instances, whereas instability in other solvers can obscure these signals.

In summary, although the GenBench-MILP framework is solver-agnostic, the quality of its evaluation results is closely tied to the stability of the solver’s internal strategies. State-of-the-art commercial solvers like Gurobi provide a more precise and reliable benchmark for our evaluation framework. At the same time, these experiments reveal an additional potential application of GenBench-MILP: as a diagnostic tool to analyze and compare the internal stability and dynamic behavior of different solvers.